Poochinapan and Wongsaijai *Advances in Continuous and Discrete Models* (2023) 2023:13
https://doi.org/10.1186/s13662-023-03760-w

Advances in Continuous and Discrete Models

RESEARCH Open Access

# Novel advances in high-order numerical algorithm for evaluation of the shallow water wave equations

Kanyuta Poochinapan[1,2] and Ben Wongsaijai[1,2*]

*Correspondence:
ben.wongsaijai@gmail.com
[1] Advanced Research Center for Computational Simulation, Chiang Mai University, Chiang Mai, 50200, Thailand
[2] Department of Mathematics, Faculty of Science, Chiang Mai University, Chiang Mai, 50200, Thailand

**Abstract**

In this paper, we propose a high-order nonlinear algorithm based on a finite difference method modification to the regularized long wave equation and the Benjamin–Bona–Mahony–Burgers equation subject to the homogeneous boundary. The consequence system of nonlinear equations typically trades with high computation burden. This dilemma can be overcome by establishing a fast numerical algorithm procedure without a reduction of numerical accuracy. The proposed algorithm forms a linear system with constant coefficient matrix at each time step and produces numerical solutions, which remarkably gains many computational advantages. In terms of analysis, a priori estimation for the numerical solution is derived to obtain the convergence and stability analysis. Additionally, the algorithm is globally mass preserving to avoid nonphysical behavior. Two benchmarks, including a single solitary wave to both equations, are given to validate the applicability and accuracy of the proposed method. Numerical results are obtained and compared to other approaches available in the literature. From the comparisons it is clear that the proposed approach produces accurate and precise results at low computational cost. Besides, the proposed scheme is applied to study the effect of the viscous term on a single solitary wave. It is shown that the viscous term results in the amplitude and width of the initial condition but not in its velocities in the case of a single solitary wave. As a consequence, theoretical and numerical findings provide a new area to investigate and expand the high-order algorithm for the family of wave equations.

**Keywords:** Finite difference method; Compact difference operator; RLW equation; BBM–Burgers equation; Convergence; Stability

## 1 Introduction

The Benjamin–Bona–Mahony (BBM) or regularized long-wave (RLW) equation

$$u_t - \mu u_{xxt} + u_x + \gamma u u_x = 0 \tag{1}$$

where $\mu$ is a positive constant and $\gamma$ is a nonzero real constant, is one of the intensive study mathematical models for the nonlinear dispersive wave, which was formulated by Peregrine [1, 2]. The RLW equation is an improvement of the Korteweg-de Vries (KdV) equation [3, 4] for modeling long surface gravity waves of small amplitude to study nonlinear dispersion. Based on large empirical applications on ion-acoustic and magnetohydrodynamics waves in plasma, longitudinal dispersive waves in elastic rods, pressure waves in liquid–gas bubble mixtures, and rotating flow down a tube, many scholars have technically and numerically obtained the mathematical principle for the RLW equation. The existence and uniqueness of a solution to the RLW equations were proved by Bona and Bryant [5]. Undular bores are usually characterized as the transition between two separate states when studying them. For example, the occurrence of internal undular bores in the density-stratified waters of the coastal ocean was studied in [6, 7], and the waveforms in the cloud formation in the atmospheric boundary were given by Rottman and Grimshaw [8]. Further, many publications [9–20] have developed numerical solutions to the RLW and related equations.

Over several years, there is a growing interest in nonlinear wave phenomena computing. The Tsunami wave, which has a huge amplitude and a long wavelength, is a study example. Shallow-water and equatorial wave considerations are commonly studied in oceanography and atmospheric science. Furthermore, equatorial waves are of particular importance because they play an important role in the evolution of many weather and climate phenomena, e.g., tropical cyclone genesis and Walker circulations. Nonlinear partial differential equations govern a variety of shallow water wave phenomena, which are not only the KdV and RLW equations, but also the Burgers equation. To fully represent real-world conditions, it is essential to consider dissipative processes when defining the propagation of small-amplitude long waves in a nonlinear dispersive medium. The processes that cause wave degradation are mostly complex and little known. The Benjamin–Bona–Mahony–Burgers (BBM–Burgers) equation [21] has gained popularity because of the need to add dissipation to nonlinearity and dispersion in modeling unidirectional propagation of planar waves. The BBM–Burgers equation is

$$u_t - \mu u_{xxt} - \alpha u_{xx} + u_x + \gamma u u_x = 0, \tag{2}$$

where $\mu$ and $\alpha$ are positive constants, and $\gamma$ is a nonzero real constant. Also, the BBM–Burgers equation has been widely studied by many researchers. In [22] the traveling wave solutions of the BBM–Burgers equation were obtained by using the $(\frac{G'}{G})$-expansion method. The Lie classical symmetries and conservative laws for a family of the BBM–Burgers equation were derived in [23]. Bell-shaped and kink-shaped solutions of the generalized BBM-Burgers were found by the improved system technique [24]. Much effort has been devoted to the development of computational methods for the BBM–Burgers equation, including the finite difference methods (FDMs) [25–30], Adomian's decomposition methods [31], meshfree methods [32, 33], collocation method [34], B-spline quasi-interpolation [35], and Galerkin cubic B-spline finite element method [36].

Due to the number of publications on numerical studies on both RLW and BBM–Burgers equations, much effort has been made to develop effective FDMs [17–19, 25–30]. Most of the previous experiments, however, have the second order of precision in time and space. In the literature the development of high-order schemes is very scarce. To the best of our knowledge, there is only on work providing a fourth-order FDM based on the Richardson extrapolation technique [30]. In this paper, we aim to fill this gap by constructing a high-order FDM combining the compact difference operators and the Richardson extrapolation technique. Consider the following initial boundary value problem of the

BBM–Burgers equation (2) under the physical boundary conditions

$$u(x,t) \to 0 \quad \text{and} \quad \partial_x^n u(x,t) \to 0 \quad \text{as } x \to \pm\infty, t \in [0,T], n \in \mathbb{N}_+, \tag{3}$$

with the initial condition

$$u(x,0) = u_0(x), \quad x \in [x_L, x_R], \tag{4}$$

where $u_0$ is a known smooth function. It is simple to demonstrate that problem (2)–(4) obeys the mass-conservative rule

$$I_1(t) = \int_{x_L}^{x_R} u(x,t)\,dx = \int_{x_L}^{x_R} u(x,0)\,dx = I_1(0) \tag{5}$$

in asymptotic boundary conditions.

The remaining part of the paper is structured as follows: The novel complex implicit finite difference scheme (FDS) for the BBM–Burgers equation (2) with initial and boundary conditions (3)–(4) is described in the following section. Section 3 contains brief preliminary results and the proof of the mass-preserving property of the new scheme. The convergence and stability of the proposed scheme is also established. The iterative algorithm for solving nonlinear implicit schemes is defined in this analysis by the constant pentadiagonal matrix. Section 4 presents several numerical findings to help and verify the theoretical study, as well as to demonstrate the success of the proposed scheme. Further, the effect of a linear viscous term and long-time behavior are also investigated. Finally, in the final segment, we conclude our paper with a brief discussion.

## 2 A novel finite difference scheme

In this part, we present a finite difference method for solving the initial boundary value problem (2)–(4). We begin by introducing the solution domain and its grid to construct our numerical scheme. Let $[x_L, x_R]$ denote the computational domain discretized by the sequence $\{x_i\}_{i=0}^{M} \subset [x_L, x_R]$, where $x_i = x_L + ih$ with $h = (x_R - x_L)/M$ a uniform step size for a positive fixed integer $M$. For the time domain, we discretized it uniformly by $t_n = n\tau$. We use the notation $u_i^n$ to represent the approximate value of a function $u$ at a grid point $(x_L + ih, n\tau)$. Under hypothesis (3), it is logical to let $u_{-1} = u_0 = u_1 = 0$ and $u_{M-1} = u_M = u_{M+1} = 0$. Then we denote

$$Z_{h,0} = \left\{u = (u_i) | u_{-1} = u_0 = u_1 = u_{M-1} = u_M = u_{M+1} = 0\right\}.$$

For clarity, we introduce the following notations:

$$\delta_t\left(u_i^n\right) = \frac{u_i^{n+1} - u_i^n}{\tau}, \qquad \delta_{\bar{t}}\left(u_i^n\right) = \frac{u_i^n - u_i^{n-1}}{\tau}, \qquad \delta_{t\bar{t}}^{(2)}\left(u_i^n\right) = \frac{u_i^{n+1} - 2u_i^n + u_i^{n-1}}{\tau^2},$$
$$\delta_x\left(u_i^n\right) = \frac{u_{i+1}^n - u_i^n}{h}, \qquad \delta_{\bar{x}}\left(u_i^n\right) = \frac{u_i^n - u_{i-1}^n}{h}, \qquad \delta_{\hat{x}}\left(u_i^n\right) = \frac{u_{i+1}^n - u_{i-1}^n}{2h},$$
$$\delta_{\ddot{x}}\left(u_i^n\right) = \frac{u_{i+2}^n - u_{i-2}^n}{4h}, \qquad \delta_{x\bar{x}}^{(2)}\left(u_i^n\right) = \delta_x\delta_{\bar{x}}\left(u_i^n\right), \qquad \delta_{\hat{x}\hat{x}}^{(2)}\left(u_i^n\right) = \delta_{\hat{x}}\delta_{\hat{x}}\left(u_i^n\right),$$
$$\delta_{xx\bar{x}\bar{x}}^{(4)}\left(u_i^n\right) = \delta_x\delta_x\delta_{\bar{x}}\delta_{\bar{x}}\left(u_i^n\right),$$

and

$$\mathcal{A}_x(u_i^n) = \left(1 + \frac{h^2}{6}\delta_{x\bar{x}}^{(2)}\right)u_i^n,$$

$$\mathcal{A}_t(u_i^n) = \left(1 + \frac{\tau^2}{6}\delta_{t\bar{t}}^{(2)}\right)u_i^n,$$

$$\mathcal{L}_x(u_i^n) = \left(1 - \frac{h^2}{12}\delta_{x\bar{x}}^{(2)}\right)u_i^n.$$

The discrete $L_2$ inner product and corresponding discrete $L_2$-norm for functions $u, v \in Z_{h,0}$ can be specified by

$$\langle u, v\rangle = h\sum_{i=1}^{M-1} u_i v_i \quad \text{and} \quad \|u\| = \langle u, u\rangle^{\frac{1}{2}},$$

respectively, and the $L_\infty$-norm is specified by $\|u\|_\infty = \max_{1\le i\le M}|u_i|$.

Now we are ready to design a higher-order FDM for the BBM–Burgers equation (2). The key idea is to implement an efficient high-order scheme for the RLW equation (1) and apply the Richardson extrapolation technique for the viscous term. According to Taylor's expansion, we recall the following compact difference operators [37, 38]:

$$u_x|_{(x_i,t^n)} = \mathcal{A}_x^{-1}\delta_{\hat{x}}(u_i^n) + O(h^4),$$

$$u_t|_{(x_i,t^n)} = \mathcal{A}_t^{-1}\delta_{\hat{t}}(u_i^n) + O(\tau^4).$$

In addition, by the Richardson extrapolation we have

$$\begin{aligned} u_{xx}|_{(x_i,t^n)} &= \delta_{x\bar{x}}^{(2)}(u_i^n) - \frac{h^2}{12}u_{xxxx}|_{(x_i,t^n)} + O(h^4) \\ &= \delta_{x\bar{x}}^{(2)}(u_i^n) - \frac{h^2}{12}\delta_{xx\bar{x}\bar{x}}^{(4)}(u_i^n) + O(h^4) \\ &= \mathcal{L}_x\delta_{x\bar{x}}^{(2)}(u_i^n) + O(h^4). \end{aligned} \tag{6}$$

After discretizing equation (1) in time and space, we obtain the following definition of an FDS and an algorithm for equation (1):

$$\mathcal{A}_t^{-1}\delta_{\hat{t}}(u_i^n) - \mu\mathcal{A}_t^{-1}\mathcal{L}_x\delta_{x\bar{x}}^{(2)}\delta_{\hat{t}}(u_i^n) + \mathcal{A}_x^{-1}\delta_{\hat{x}}(u_i^n) + \frac{\gamma}{2}\mathcal{A}_x^{-1}\delta_{\hat{x}}\left[(u_i^n)^2\right] = 0.$$

Applying the above approximation with the operator $\mathcal{A}_x\mathcal{A}_t$ and noticing that

$$\mathcal{A}_x\mathcal{L}_x\delta_{x\bar{x}}^{(2)}\delta_{\hat{t}}(u_i^n) = \mathcal{A}_x\delta_{x\bar{x}}^{(2)}\delta_{\hat{t}}(u_i^n) - \frac{h^2}{12}\delta_{xx\bar{x}\bar{x}}^{(4)}\delta_{\hat{t}}(u_i^n) + O(\tau^4 + h^4),$$

we obtain the following detailed numerical scheme for the RLW equation:

$$\mathcal{A}_x\delta_{\hat{t}}(u_i^n) - \mu\mathcal{A}_x\delta_{x\bar{x}}^{(2)}\delta_{\hat{t}}(u_i^n) + \mu\frac{h^2}{12}\delta_{xx\bar{x}\bar{x}}^{(4)}\delta_{\hat{t}}(u_i^n) + \mathcal{A}_t\delta_{\hat{x}}(u_i^n) + \frac{\gamma}{2}\mathcal{A}_t\delta_{\hat{x}}\left[(u_i^n)^2\right] = 0. \tag{7}$$

Finally, we use the Crank–Nicolson/Adams–Bashforth technique to approximate the viscous term $-\alpha u_{xx}$ described in equation (6) as

$$u_{xx}|_{(x_i,t^n)} = \mathcal{L}_x\delta_{x\bar{x}}^{(2)}\left(\bar{u}_i^n\right) + O\left(\tau^2 + h^4\right).$$

Then, for the initial boundary value problem (2)–(4), we suggest the three-level difference scheme

$$\begin{aligned} &\mathcal{A}_x\delta_{\hat{t}}\left(u_i^n\right) - \mu\mathcal{A}_x\delta_{x\bar{x}}^{(2)}\delta_{\hat{t}}\left(u_i^n\right) + \mu\frac{h^2}{12}\delta_{xx\bar{x}\bar{x}}^{(4)}\delta_{\hat{t}}\left(u_i^n\right) \\ &\quad - \alpha\mathcal{L}_x\delta_{x\bar{x}}^{(2)}\bar{u}_i^n + \mathcal{A}_t\delta_{\hat{x}}\left(u_i^n\right) + \frac{\gamma}{2}\mathcal{A}_t\delta_{\hat{x}}\left[\left(u_i^n\right)^2\right] = 0 \end{aligned} \tag{8}$$

with the initial condition

$$u_i^0 = u_0(x_i), \quad 0 \le i \le M, \tag{9}$$

and the boundary conditions

$$u_0^n = u_M^n = 0, \qquad \delta_{\hat{x}}\left(u_0^n\right) = \delta_{\hat{x}}\left(u_M^n\right) = 0, \qquad \delta_{x\bar{x}}^{(2)}\left(u_0^n\right) = \delta_{x\bar{x}}^{(2)}\left(u_M^n\right) = 0, \quad 1 \le n \le N. \tag{10}$$

It is worth mentioning that by using the Taylor expansion we can see from the above reformulations that scheme (7) achieves the truncation error of order $O(\tau^2 + h^4)$ if the estimated function is sufficiently smooth, whereas the truncation error becomes $O(\tau^4 + h^4)$ when $\alpha = 0$. Because the algorithm employs a three-level estimation of time together with the initial conditions $u^0$, we need $u^1$ as known conditions. As a result, we first choose a two-level scheme with a second-order accuracy process. For this reason, we can determine $u^1$ based on the fourth-order two-level scheme [30].

## 3 Main results

In this section, we address the convergence and stability for our numerical scheme. We will denote by $C$ as a generic constant independent of step sizes $h$ and $\tau$. To demonstrate the boundedness, convergence, and stability of our numerical solutions, we need the following lemmas. Lemma 1 can be directly determined by summation by parts. So the proofs are omitted.

**Lemma 1** *Let $w, v \in Z_{h,0}$ be mesh functions. Then we have*

1. $\langle\delta_{\hat{x}}w, v\rangle = -\langle w, \delta_{\hat{x}}v\rangle$;
2. $\langle\delta_{x\bar{x}}^{(2)}w, v\rangle = \langle w, \delta_{x\bar{x}}^{(2)}v\rangle = -\langle\delta_x w, \delta_x v\rangle$;
3. $\langle\delta_{xx\bar{x}\bar{x}}^{(4)}w, v\rangle = \langle w, \delta_{xx\bar{x}\bar{x}}^{(4)}v\rangle = -\langle\delta_{x\bar{x}}^{(2)}w, \delta_{x\bar{x}}^{(2)}v\rangle$.

*Moreover, we have*

$$\langle\delta_{\hat{x}}w, w\rangle = 0, \qquad \left\langle\delta_{x\bar{x}}^{(2)}w, w\right\rangle = -\|\delta_x w\|^2, \quad \textit{and} \quad \left\langle\delta_{xx\bar{x}\bar{x}}^{(4)}w, w\right\rangle = \left\|\delta_{x\bar{x}}^{(2)}w\right\|^2.$$

**Lemma 2** *Let $u \in Z_{h,0}$ be a mesh function. Then we have*

(i) $\langle\mathcal{A}_x u, u\rangle = \|u\|^2 - \frac{h^2}{6}\|\delta_x u\|^2$;
(ii) $\langle\mathcal{A}_x\delta_{x\bar{x}}^{(2)}u, u\rangle = -\|\delta_x u\|^2 + \frac{h^2}{6}\|\delta_{x\bar{x}}^{(2)}u\|^2$;
(iii) $\langle\mathcal{L}_x\delta_{x\bar{x}}^{(2)}u, u\rangle = -\|\delta_x u\|^2 - \frac{h^2}{12}\|\delta_{x\bar{x}}^{(2)}u\|^2$.

*Proof* Let $u \in Z_{h,0}$. By Lemma 1 we have

$$\langle \mathcal{A}_x u, u\rangle = \|u\|^2 + \frac{h^2}{6}\langle \delta_{x\bar{x}}^{(2)} u, u\rangle = -\|u\|^2 - \frac{h^2}{6}\|\delta_x u\|^2.$$

Similarly, the rest can be obtained applying Lemma 1. □

**Lemma 3** *Let $u, v \in Z_{h,0}$ be mesh functions. Then, for any $\epsilon_1, \epsilon_2 \in \mathbb{R}^+$, we have the following estimates*:

(i) $\langle \mathcal{A}_x u, v\rangle \leq \frac{\epsilon_1}{2}\|u\|^2 + \frac{1}{2\epsilon_1}\|v\|^2 + \frac{\epsilon_2 h^2}{12}\|\delta_x u\|^2 + \frac{h^2}{12\epsilon_2}\|\delta_x v\|^2$;

(ii) $\langle \mathcal{A}_x \delta_{x\bar{x}}^{(2)} u, v\rangle \leq \frac{\epsilon_1}{2}\|\delta_x u\|^2 + \frac{1}{2\epsilon_1}\|\delta_x v\|^2 + \frac{\epsilon_2 h^2}{12}\|\delta_{x\bar{x}}^{(2)} u\|^2 + \frac{h^2}{12\epsilon_2}\|\delta_{x\bar{x}}^{(2)} v\|^2$;

(iii) $\langle \mathcal{L}_x \delta_{x\bar{x}}^{(2)} u, v\rangle \leq \frac{\epsilon_1}{2}\|\delta_x u\|^2 + \frac{1}{2\epsilon_1}\|\delta_x v\|^2 + \frac{\epsilon_2 h^2}{24}\|\delta_{x\bar{x}}^{(2)} u\|^2 + \frac{h^2}{24\epsilon_2}\|\delta_{x\bar{x}}^{(2)} v\|^2$.

*Proof* Let $u \in Z_{h,0}$ and $\epsilon_1, \epsilon_2 \in \mathbb{R}^+$. By applying Lemma 1 and Young's inequality we have

$$\begin{aligned}
\langle \mathcal{A}_x u, v\rangle &= \langle u, v\rangle - \frac{h^2}{6}\langle \delta_x u, \delta_x v\rangle \\
&\leq \|u\|\|v\| + \frac{h^2}{6}\|\delta_x u\|\|\delta_x v\| \\
&\leq \frac{\epsilon_1}{2}\|u\|^2 + \frac{1}{2\epsilon_1}\|v\|^2 + \frac{\epsilon_2 h^2}{12}\|\delta_x u\|^2 + \frac{h^2}{12\epsilon_2}\|\delta_x v\|^2.
\end{aligned}$$

Likewise, the rest can be obtained applying Lemma 1 and Young's inequality. □

**Lemma 4** (See [39]) *Let $u \in Z_{h,0}$ be a mesh function. Then we have*

$$\|\delta_x u\| \leq \frac{4}{h^2}\|u\|^2 \quad \textit{and} \quad \big\|\delta_{x\bar{x}}^{(2)} u\big\| \leq \frac{4}{h^2}\|\delta_x u\|^2.$$

**Lemma 5** (Discrete Sobolev's inequality [40]) *There exist two constants $C_1$ and $C_2$ such that*

$$\big\|u^n\big\|_\infty \leq C_1\big\|u^n\big\| + C_2\big\|u_x^n\big\|.$$

**Lemma 6** (Discrete Gronwall inequality [40]) *Suppose that $\omega(k)$ and $\rho(k)$ are nonnegative functions and $\rho(k)$ is a nondecreasing function. If $C > 0$ and*

$$\omega(k) \leq \rho(k) + C\tau\sum_{l=0}^{k-1}\omega(l) \quad \forall k,$$

*then*

$$\omega(k) \leq \rho(k)e^{C\tau k} \quad \forall k.$$

We first observe that our numerical algorithm preserves the mass quantity.

**Theorem 7** *Suppose that $u^n \in Z_{h,0}$. Then scheme (8)–(10) is conservative in the sense that*

$$I_{1,1}^n = \frac{h}{2}\sum_{i=1}^{M-1}\left(u_i^{n+1} + u_i^n\right) = I_{1,1}^{n-1} = \cdots = I_{1,1}^0. \tag{11}$$

*Proof* Multiplying equation (8) by $h$ and summing up for $i$ from 0 to $M-1$, we get

$$h\sum_{i=1}^{M-1}\mathcal{A}_x\delta_{\hat{t}}(u_i^n) - \mu h\sum_{i=1}^{M-1}\mathcal{A}_x\delta_{x\bar{x}}^{(2)}\delta_{\hat{t}}(u_i^n) + \mu\frac{h^2}{12}h\sum_{i=1}^{M-1}\delta_{xx\bar{x}\bar{x}}^{(4)}\delta_{\hat{t}}(u_i^n)$$
$$-\alpha h\sum_{i=1}^{M-1}\mathcal{L}_x\delta_{x\bar{x}}^{(2)}(\bar{u}_i^n) + h\sum_{i=1}^{M-1}\mathcal{A}_t\delta_{\hat{x}}(u_i^n) + \frac{\gamma}{2}h\sum_{i=1}^{M-1}\mathcal{A}_t\delta_{\hat{x}}\big[(u_i^n)^2\big] = 0.$$

Considering the boundary conditions and $u^n \in Z_{h,0}$, we observe that

$$h\sum_{i=1}^{M-1}\mathcal{A}_x\delta_{\hat{t}}(u_i^n) = h\sum_{i=1}^{M-1}\delta_{\hat{t}}(u_i^n) + \frac{h^3}{6}\sum_{i=1}^{M-1}\delta_{x\bar{x}}^{(2)}\delta_{\hat{t}}(u_i^n)$$
$$= h\sum_{i=1}^{M-1}\delta_{\hat{t}}(u_i^n).$$

Similarly, the other terms vanish by applying the boundary conditions, which yield

$$h\sum_{i=1}^{M-1}\delta_{\hat{t}}(u_i^n) = h\sum_{i=1}^{M-1}\frac{u_i^{n+1}-u_i^{n-1}}{2\tau} = 0,$$

which gives equation (11), completing the proof. □

The next theorem shows that our numerical solution is bounded for any given initial function $u_0$.

**Theorem 8** (Boundedness) *Suppose $u^n \in Z_{h,0}$ and $u_0 \in C^2[x_L,x_R]$. If $\tau$ and $h$ are sufficiently small, then the solution $u^n$ satisfies*

$$\|u^n\| \le C, \qquad \|\delta_x u^n\| \le C, \quad \textit{and} \quad \|u^n\|_\infty \le C$$

*for $n = 1,2,\ldots,N$.*

*Proof* To prove the boundedness, we use the mathematical induction by assuming that

$$\|u^k\| \le C, \qquad \|\delta_x u^k\| \le C, \quad \text{and} \quad \|u^k\|_\infty \le C \tag{12}$$

for $k = 1,2,\ldots,n$. Taking the inner product in equation (8) with $2\bar{u}^n$ (i.e., $u^{n+1}+u^{n-1}$), we get

$$\langle\mathcal{A}_x\delta_{\hat{t}}u^n, 2\bar{u}^n\rangle - \mu\langle\mathcal{A}_x\delta_{x\bar{x}}^{(2)}\delta_{\hat{t}}u^n, 2\bar{u}^n\rangle + \frac{\mu h^2}{12}\langle\delta_{xx\bar{x}\bar{x}}^{(4)}\delta_{\hat{t}}u^n, 2\bar{u}^n\rangle - \alpha\langle\mathcal{L}_x\delta_{x\bar{x}}^{(2)}\bar{u}^n, 2\bar{u}^n\rangle$$
$$+\langle\mathcal{A}_t\delta_{\hat{x}}u^n, 2\bar{u}^n\rangle + \frac{\gamma}{2}\langle\mathcal{A}_t\delta_{\hat{x}}\big[(u^n)^2\big], 2\bar{u}^n\rangle = 0. \tag{13}$$

According to Lemmas 1 and 2, we have

$$\frac{1}{2\tau}\big(\|u^{n+1}\|^2 - \|u^{n-1}\|^2\big) + \frac{s_1}{2\tau}\big(\|\delta_x u^{n+1}\|^2 - \|\delta_x u^{n-1}\|^2\big)$$

$$
\begin{aligned}
&-\frac{\mu h^2}{24\tau}\left(\left\|\delta_{x\bar{x}}^{(2)}u^{n+1}\right\|^2-\left\|\delta_{x\bar{x}}^{(2)}u^{n-1}\right\|^2\right)\\
&+\alpha\left\|\delta_x\bar{u}^n\right\|^2+\frac{\alpha h^2}{12}\left\|\delta_{x\bar{x}}^{(2)}\bar{u}^n\right\|^2+\left\langle\mathcal{A}_t\delta_{\hat{x}}u^n,2\bar{u}^n\right\rangle+\frac{\gamma}{2}\left\langle\mathcal{A}_t\delta_{\hat{x}}\left[\left(u^n\right)^2\right],2\bar{u}^n\right\rangle=0, \qquad (14)
\end{aligned}
$$

where $s_1=\mu-\frac{h^2}{6}$. By Lemma 1, the Cauchy–Schwarz inequality, and assumption (12) we have

$$
\begin{aligned}
\left\langle\mathcal{A}_t\delta_{\hat{x}}u^n,2\bar{u}^n\right\rangle&=\left\langle\delta_{\hat{x}}u^n,2\bar{u}^n\right\rangle+\frac{\tau^2}{6}\left\langle\delta_{t\bar{t}}^{(2)}\delta_{\hat{x}}u^n,2\bar{u}^n\right\rangle\\
&\le\left\|\delta_{\hat{x}}u^n\right\|^2+\left\|\bar{u}^n\right\|^2+\frac{1}{6}\left(\left\|\delta_{\hat{x}}u^{n+1}\right\|^2+2\left\|\delta_{\hat{x}}u^n\right\|^2+\left\|\delta_{\hat{x}}u^{n-1}\right\|^2+3\left\|\bar{u}^n\right\|^2\right)\\
&=\frac{1}{6}\left\|\delta_{\hat{x}}u^{n+1}\right\|^2+\frac{4}{3}\left\|\delta_{\hat{x}}u^n\right\|^2+\frac{1}{6}\left\|\delta_{\hat{x}}u^{n-1}\right\|^2+\frac{3}{2}\left\|\bar{u}^n\right\|^2 \qquad (15)
\end{aligned}
$$

and

$$
\begin{aligned}
\left\langle\mathcal{A}_t\delta_{\hat{x}}\left[\left(u^n\right)^2\right],2\bar{u}^n\right\rangle&=\left\langle\delta_{\hat{x}}\left[\left(u^n\right)^2\right],2\bar{u}^n\right\rangle+\frac{\tau^2}{6}\left\langle\delta_{t\bar{t}}^{(2)}\delta_{\hat{x}}\left[\left(u^n\right)^2\right],2\bar{u}^n\right\rangle\\
&=-\left\langle\left[\left(u^n\right)^2\right],2\delta_{\hat{x}}\bar{u}^n\right\rangle-\frac{\tau^2}{6}\left\langle\delta_{t\bar{t}}^{(2)}\left[\left(u^n\right)^2\right],2\delta_{\hat{x}}\bar{u}^n\right\rangle\\
&=-2h\sum_{i=1}^{M-1}\left[\left(u_i^n\right)^2\right]\delta_{\hat{x}}\left(\bar{u}_i^n\right)-\frac{1}{3}\sum_{i=1}^{M-1}\left[\left(u_i^{n+1}\right)^2-2\left(u_i^n\right)^2+\left(u_i^{n-1}\right)^2\right]\delta_{\hat{x}}\left(\bar{u}_i^n\right)\\
&\le C\left(\left\|u^{n-1}\right\|^2+\left\|u^n\right\|^2+\left\|u^{n+1}\right\|^2+\left\|\delta_{\hat{x}}\bar{u}^n\right\|^2\right). \qquad (16)
\end{aligned}
$$

Since $u^n\in Z_{h,0}$, applying the Cauchy–Schwarz inequality, we have

$$
\left\|\delta_{\hat{x}}u^n\right\|^2=\frac{1}{4}\left\|\delta_xu^n+\delta_{\bar{x}}u^n\right\|^2\le\frac{1}{2}\left(\left\|\delta_xu^n\right\|^2+\left\|\delta_{\bar{x}}u^n\right\|^2\right)=\left\|\delta_xu^n\right\|^2 \qquad (17)
$$

and

$$
\left\|\bar{u}^n\right\|^2=\frac{1}{4}\left\|u^{n+1}+u^{n-1}\right\|^2\le\frac{1}{2}\left(\left\|u^{n+1}\right\|^2+\left\|u^{n-1}\right\|^2\right). \qquad (18)
$$

Substituting equations (15)–(18) into equation (14), we get

$$
\begin{aligned}
&\left(\left\|u^{n+1}\right\|^2-\left\|u^{n-1}\right\|^2\right)+s_1\left(\left\|\delta_xu^{n+1}\right\|^2-\left\|\delta_xu^{n-1}\right\|^2\right)-\frac{\mu h^2}{12}\left(\left\|\delta_{x\bar{x}}^{(2)}u^{n+1}\right\|^2-\left\|\delta_{x\bar{x}}^{(2)}u^{n-1}\right\|^2\right)\\
&\quad\le C\tau\left(\left\|u^{n-1}\right\|^2+\left\|u^n\right\|^2+\left\|u^{n+1}\right\|^2+\left\|\delta_xu^{n-1}\right\|^2+\left\|\delta_xu^n\right\|^2+\left\|\delta_xu^{n+1}\right\|^2\right). \qquad (19)
\end{aligned}
$$

If $h$ is sufficiently small such that $4\mu-h^2>0$, then by Lemma 4 then the above equation can be estimated as

$$
\begin{aligned}
&\left(\left\|u^{n+1}\right\|^2-\left\|u^{n-1}\right\|^2\right)+\left(\left\|\delta_xu^{n+1}\right\|^2-\left\|\delta_xu^{n-1}\right\|^2\right)\\
&\quad\le C\tau\left(\left\|u^{n-1}\right\|^2+\left\|u^n\right\|^2+\left\|u^{n+1}\right\|^2+\left\|\delta_xu^{n-1}\right\|^2+\left\|\delta_xu^n\right\|^2+\left\|\delta_xu^{n+1}\right\|^2\right).
\end{aligned}
$$

Here we let

$$
B^n\equiv\left(\left\|u^n\right\|^2+\left\|u^{n-1}\right\|^2\right)+\left(\left\|\delta_xu^n\right\|^2+\left\|\delta_xu^{n-1}\right\|^2\right).
$$

Then equation (19) can be rewritten as

$$B^{n+1} - B^n \leq \tau C\big(B^{n+1} + B^n\big).$$

If $\tau$ is sufficiently small, such that $\tau \leq \frac{k-2}{kC}$ and $k > 2$, then

$$B^{n+1} \leq \frac{(1+\tau C)}{(1-\tau C)} B^n \leq (1+\tau kC)B^n \leq \exp(kCT)B^0.$$

Hence

$$\|u^{n+1}\|^2 \leq C \quad \text{and} \quad \|\delta_x u^{n+1}\|^2 \leq C.$$

We complete the proof by using Lemma 5 to obtain $\|u^{n+1}\|_\infty \leq C$. □

In this section, we show that scheme (8)–(10) is solvable. This ensures that our numerical solution exists and is unique. We use the Browder fixed point to demonstrate the existence of a solution; the proof will be based on the theorem. Here we recall the Browder fixed point theorem.

**Lemma 9** (Browder fixed point theorem) *Let $H$ be a finite-dimensional inner product space. Suppose that $g: H \to H$ is continuous and there exists $\varepsilon > 0$ such that $\langle g(v), v\rangle > 0$ for all $x \in H$ with $\|x\| = \varepsilon$. Then there exists $x^* \in H$ such that $g(x^*) = 0$ and $\|x^*\| \leq \varepsilon$.*

**Theorem 10** *If $\tau$ is sufficiently small, then scheme (8)–(10) is solvable.*

*Proof* To prove the theorem, we proceed by mathematical induction. We assume that $u^0, u^1, \dots, u^n$ satisfy scheme (8)–(10) for $1 \leq n \leq N-1$. Indeed, $u^1$ can be computed by an available fourth-order method as we mentioned before. Next, we prove that there exists $u^{n+1}$ satisfying equations (8)–(10). Define the operator $g: Z_{h,0} \to Z_{h,0}$ as follows:

$$\begin{aligned} g(v) &= \mathcal{A}_x\big(v - u^{n-1}\big) - \mu \mathcal{A}_x \delta_{x\bar{x}}^{(2)}\big(v - u^{n-1}\big) + \mu \frac{h^2}{12}\delta_{xx\bar{x}\bar{x}}^{(4)}\big(v - u^{n-1}\big) \\ &\quad - \tau\alpha \mathcal{L}_x \delta_{x\bar{x}}^{(2)}\big(v + u^{n-1}\big) + 2\tau\delta_{\hat{x}}\big(u^n\big) + \frac{\tau}{3}\big(v - 2u^n + u^{n-1}\big) \\ &\quad + \tau\gamma\delta_{\hat{x}}\big[\big(u^n\big)^2\big] + \gamma\frac{\tau}{6}\delta_{\hat{x}}\big[(v)^2 - 2\big(u^n\big)^2 + \big(u^{n-1}\big)^2\big]. \end{aligned} \tag{20}$$

To apply the Browder fixed point theorem, we need to show that there exists $\varepsilon > 0$ such that $\langle g(v), v\rangle > 0$ for all $v \in Z_{h,0}$ with $\|v\| = \varepsilon$. Let us consider

$$\begin{aligned} \big\langle g(v), v\big\rangle &= \|v\|^2 + s_1\|\delta_x v\|^2 - \mu\frac{h^2}{12}\big\|\delta_{x\bar{x}}^{(2)} v\big\|^2 + \tau\alpha\left(\|\delta_x v\|^2 + \frac{h^2}{12}\big\|\delta_{x\bar{x}}^{(2)} v\big\|^2\right) \\ &\quad + \frac{\tau}{3}\|v\|^2 + \gamma\frac{\tau}{6}\big\langle\delta_{\hat{x}}[v]^2, v\big\rangle - \big\langle \mathcal{A}_x u^{n-1}, v\big\rangle - \mu\big\langle \mathcal{A}_x\delta_{x\bar{x}}^{(2)} u^{n-1}, v\big\rangle + \mu\frac{h^2}{12}\big\langle\delta_{xx\bar{x}\bar{x}}^{(4)} u^{n-1}, v\big\rangle \\ &\quad - \tau\alpha\big\langle \mathcal{L}_x\delta_{x\bar{x}}^{(2)} u^{n-1}, v\big\rangle + \frac{\tau}{3}\big(4\big\langle\delta_{\hat{x}} u^n, v\big\rangle + \big\langle\delta_{\hat{x}} u^{n-1}, v\big\rangle\big) \\ &\quad + \gamma\frac{\tau}{6}\big(4\big\langle\delta_{\hat{x}}\big[u^n\big]^2, v\big\rangle + \big\langle\delta_{\hat{x}}\big[u^{n-1}\big]^2, v\big\rangle\big), \end{aligned} \tag{21}$$

where we use Lemmas 1 and 2. We first estimate the term $\frac{\tau}{6}\langle\delta_{\hat{x}}[v]^2, v\rangle$:

$$\frac{\tau}{6}\langle\delta_{\hat{x}}[v]^2, v\rangle = -\frac{h\tau}{6}\sum_{i=1}^{M}(v_i)^2\delta_{\hat{x}}(v_i) \le \frac{\tau}{12}\|v\|_4^4 + \frac{\tau}{12}\|\delta_x v\|^2, \tag{22}$$

where $\|\cdot\|_4$ is the usual $L_4$-norm. Applying Lemma 3, we have the following estimates:

$$\begin{aligned}
&\langle\mathcal{A}_x u^{n-1}, v\rangle \le C\bigl(\|u^{n-1}\|^2 + \|\delta_x u^{n-1}\|^2\bigr) + \frac{1}{4}\|v\|^2 + \frac{h^2}{16}\|\delta_x v\|^2,\\
&\langle\mathcal{A}_x\delta_{x\bar{x}}^{(2)} u^{n-1}, v\rangle \le C\bigl(\|\delta_x u^{n-1}\|^2 + \|\delta_{x\bar{x}}^{(2)} u^{n-1}\|^2\bigr) + \frac{1}{3}\|\delta_x v\|^2 + \frac{h^2\tau\alpha}{36\mu}\|\delta_{x\bar{x}}^{(2)} v\|^2,\\
&\langle\mathcal{L}_x\delta_{x\bar{x}}^{(2)} u^{n-1}, v\rangle \le C\bigl(\|\delta_x u^{n-1}\|^2 + \|\delta_{x\bar{x}}^{(2)} u^{n-1}\|^2\bigr) + \frac{1}{3}\|\delta_x v\|^2 + \frac{h^2}{36}\|\delta_{x\bar{x}}^{(2)} v\|^2.
\end{aligned}$$

Also, it is easy to obtain by the Cauchy–Schwarz and Young inequalities that

$$\begin{aligned}
&\langle\delta_{xx\bar{x}\bar{x}}^{(4)} u^{n-1}, v\rangle \le \frac{3\mu}{4\tau\alpha}\|\delta_{x\bar{x}}^{(2)} u^{n-1}\|^2 + \frac{\tau\alpha}{3\mu}\|\delta_{x\bar{x}}^{(2)} v\|^2,\\
&\langle\delta_{\hat{x}} u^{n-1}, v\rangle \le \|\delta_x u^{n-1}\|^2 + \frac{1}{4}\|v\|^2,\\
&\langle\delta_{\hat{x}} u^{n}, v\rangle \le 4\|\delta_x u^{n}\|^2 + \frac{1}{16}\|v\|^2.
\end{aligned}$$

In addition, applying the Cauchy–Schwarz inequality, Young's inequality, Theorem 8, and equation (17), we see that

$$\langle\delta_{\hat{x}}[u^{n-1}]^2, v\rangle = -h\sum_{i=1}^{M}(u_i^{n-1})^2\delta_{\hat{x}}(v_i) \le C\|u^{n-1}\|\cdot\|\delta_{\hat{x}} v\| \le C\|u^{n-1}\|^2 + \frac{3\alpha}{2\gamma}\|\delta_x v\|^2.$$

Similarly, we have

$$\langle\delta_{\hat{x}}[u^{n}]^2, v\rangle \le C\|u^{n}\|^2 + \frac{3\alpha}{8\gamma}\|\delta_x v\|^2. \tag{23}$$

Substituting equations (22)–(23) into equation (21) and applying Lemma 3, it follows that

$$\begin{aligned}
\langle g(v), v\rangle &\ge \frac{1}{2}\left(\|v\|^2 + \left(\mu - \frac{h^2}{3}\right)\|\delta_x v\|^2\right) - \frac{\tau}{12}\|\delta_x v\|^2 - \mu\frac{h^2}{12}\|\delta_{x\bar{x}}^{(2)} v\|^2 - \frac{\tau}{12}\|v\|_4^4\\
&\quad - C\bigl(\|u^{n-1}\|^2 + \|\delta_x u^{n-1}\|^2 + \|u^{n}\|^2 + \|\delta_x u^{n}\|^2 + \|\delta_{x\bar{x}}^{(2)} u^{n-1}\|^2\bigr)\\
&\ge \frac{1}{2}\left(\|v\|^2 + \left(\frac{\mu}{3} - \frac{h^2}{3} - \frac{\tau}{6}\right)\|\delta_x v\|^2\right) - \frac{\tau}{12}\|v\|_4^4\\
&\quad - C\bigl(\|u^{n-1}\|^2 + \|\delta_x u^{n-1}\|^2 + \|u^{n}\|^2 + \|\delta_x u^{n}\|^2 + \|\delta_{x\bar{x}}^{(2)} u^{n-1}\|^2\bigr).
\end{aligned}$$

Observe that if $h$ and $\tau$ are sufficiently small such that $2\mu \ge h^2 + \tau$, then the above estimate turns into

$$\langle g(v), v\rangle \ge \frac{1}{2}\|v\|^2 - \frac{\tau}{12}\|v\|_4^4 - C\bigl(\|u^{n-1}\|^2 + \|\delta_x u^{n-1}\|^2 + \|u^{n}\|^2 + \|\delta_x u^{n}\|^2 + \|\delta_{x\bar{x}}^{(2)} u^{n-1}\|^2\bigr)$$

$$\geq \frac{1}{2}\|v\|^2 - \frac{\tau}{12}\|v\|^4 - C\left(\left\|u^{n-1}\right\|^2 + \left\|\delta_x u^{n-1}\right\|^2 + \left\|u^n\right\|^2 + \left\|\delta_x u^n\right\|^2 + \left\|\delta_{x\bar{x}}^{(2)} u^{n-1}\right\|^2\right),$$

where we used the fact that $\|v\| \geq \|v\|_4$. Finally, if $\tau$ is sufficiently small such that

$$K := 1 - \frac{4\tau}{3}C\left(\left\|u^{n-1}\right\|^2 + \left\|\delta_x u^{n-1}\right\|^2 + \left\|u^n\right\|^2 + \left\|\delta_x u^n\right\|^2 + \left\|\delta_{x\bar{x}}^{(2)} u^{n-1}\right\|^2\right) > 0,$$

then $\langle g(v), v\rangle \geq 0$ for all $v \in Z_{h,0}$ with $\|v\| = \frac{3}{2}[\frac{1+\sqrt{K}}{\tau}]$. It follows from the Browder fixed point theorem that there exists $v^* \in Z_{h,0}$ satisfying $g(v^*) = 0$. This implies the existence of scheme (8)–(10) and thus completes the proof. □

**Theorem 11** *If $\tau$ is sufficiently small, then scheme (8)–(10) is unique.*

*Proof* Suppose that $u^{n+1}$ and $w^{n+1}$ are two solutions of scheme (8)–(10). Taking $\rho_i^{n+1} = u_i^{n+1} - w_i^{n+1}$, we arrive at

$$\begin{aligned}
&\mathcal{A}_x\left(\rho_i^{n+1}\right) - \mu\mathcal{A}_x\delta_{x\bar{x}}^{(2)}\left(\rho_i^{n+1}\right) + \mu\frac{h^2}{12}\delta_{xx\bar{x}\bar{x}}^{(4)}\left(\rho_i^{n+1}\right) - \tau\alpha\mathcal{L}_x\delta_{x\bar{x}}^{(2)}\left(\rho_i^{n+1}\right) \\
&\quad + \frac{\tau}{3}\delta_{\hat{x}}\left(\rho_i^{n+1}\right) + \frac{\gamma\tau}{3}\delta_{\hat{x}}\left[\left(u_i^{n+1}\right)^2 - \left(w_i^{n+1}\right)^2\right] = 0.
\end{aligned} \tag{24}$$

Taking the inner product of equation (24) with $\rho^{n+1}$, by Lemmas 1 and 2 we obtain

$$\left\|\rho^{n+1}\right\|^2 + s_2\left\|\delta_x\rho^{n+1}\right\|^2 + s_3\left\|\delta_{x\bar{x}}^{(2)}\rho^{n+1}\right\|^2 + \frac{\gamma\tau}{3}\left(\delta_{\hat{x}}\left[\left(u^{n+1}\right)^2 - \left(w^{n+1}\right)^2\right], \rho^{n+1}\right) = 0, \tag{25}$$

where $s_2 = \mu - \frac{h^2}{6} + \tau\alpha$ and $s_3 = -\mu\frac{h^2}{12} + \tau\alpha\frac{h^2}{12}$. As for the nonlinear term $(\delta_{\hat{x}}[(u^{n+1})^2 - (w^{n+1})^2], \rho^{n+1})$, we see that

$$\begin{aligned}
\left(\delta_{\hat{x}}\left[\left(u^{n+1}\right)^2 - \left(w^{n+1}\right)^2\right], \rho^{n+1}\right) &= -\left(\left(u^{n+1}\right)^2 - \left(w^{n+1}\right)^2, \delta_{\hat{x}}\rho^{n+1}\right) \\
&= -\left(\rho^{n+1}\left(u^{n+1} + w^{n+1}\right), \delta_{\hat{x}}\rho^{n+1}\right) \\
&\leq C\left(\left\|\rho^{n+1}\right\|^2 + \left\|\delta_x\rho^{n+1}\right\|^2\right),
\end{aligned} \tag{26}$$

where we used Lemma 1, Theorem 8, and equation (17). Using this inequality and Theorem 4, we can estimate equation (25) as

$$\left\|\rho^{n+1}\right\|^2 + s_4\left\|\delta_x\rho^{n+1}\right\|^2 + \tau\alpha\frac{h^2}{12}\left\|\delta_{x\bar{x}}^{(2)}\rho^{n+1}\right\|^2 \leq \tau C\left(\left\|\rho^{n+1}\right\|^2 + \left\|\delta_x\rho^{n+1}\right\|^2\right),$$

where $s_4 = (\frac{2\mu}{3} - \frac{h^2}{6} + \tau\alpha)$. Hence, if $\tau$ is sufficiently small such that $\min\{1, s_4\} - \tau C > 0$, then we have

$$(1 - \tau C)\left\|\rho^{n+1}\right\|^2 + (s_4 - \tau C)\left\|\delta_x\rho^{n+1}\right\|^2 + \tau\alpha\frac{h^2}{12}\left\|\delta_{x\bar{x}}^{(2)}\rho^{n+1}\right\|^2 \leq 0.$$

So $\|\rho^{n+1}\| = \|\delta_x\rho^{n+1}\| = \|\delta_{x\bar{x}}^{(2)}\rho^{n+1}\| = 0$, that is, equation (24) has only a trivial solution. Therefore scheme (8)–(10) uniquely determines $u^{n+1}$. This completes the proof. □

To prove the convergence and stability of scheme (8)–(10), let $v_i^n = v(x_i, t^n)$ be the solution to equations (2)–(4). Then the truncation error of scheme (8)–(10) can be obtained from

$$\begin{aligned} r_i^n &= \mathcal{A}_x\delta_{\hat{t}}(e_i^n) - \mu\mathcal{A}_x\delta_{x\bar{x}}^{(2)}\delta_{\hat{t}}(e_i^n) + \mu\frac{h^2}{12}\delta_{xx\bar{x}\bar{x}}^{(4)}\delta_{\hat{t}}(e_i^n) - \alpha\mathcal{L}_x\delta_{x\bar{x}}^{(2)}(\bar{e}_i^n) \\ &\quad + \mathcal{A}_t\delta_{\hat{x}}(e_i^n) + \frac{\gamma}{2}\mathcal{A}_t\delta_{\hat{x}}\big[(v_i^n)^2\big] - \frac{\gamma}{2}\mathcal{A}_t\delta_{\hat{x}}\big[(u_i^n)^2\big]. \end{aligned} \tag{27}$$

By the Taylor expansion we can easily demonstrate that $|r_i^n| = \mathcal{O}(\tau^2 + h^4)$. Furthermore, by the previous observation the truncation error becomes $\mathcal{O}(\tau^4 + h^4)$ in the case $\alpha = 0$. Now we present the convergence theorem of the present scheme.

**Theorem 12** *Assume that the solution of equations (2)–(4) is sufficiently smooth and $u^n \in Z_{h,0}$. If $\tau$ is sufficiently small, then the solution $u^n$ of scheme (8)–(10) converges to the solution of equations (2)–(4) in the sense of $\|\cdot\|_\infty$-norm with the convergence rate of order $\mathcal{O}(\tau^2 + h^4)$. More precisely, the convergence rate turns into $\mathcal{O}(\tau^4 + h^4)$ in the case $\alpha = 0$.*

*Proof* Taking the inner product of equation (27) with $2\bar{e}^n$ (i.e., $e^{n+1} + e^{n-1}$) and using Lemma 1, we obtain

$$\begin{aligned} &\frac{1}{2\tau}\big(\|e^{n+1}\|^2 - \|e^{n-1}\|^2\big) + \frac{s_1}{2\tau}\big(\|\delta_x e^{n+1}\|^2 - \|\delta_x e^{n-1}\|^2\big) - \frac{\mu h^2}{24\tau}\big(\|\delta_{x\bar{x}}^{(2)} e^{n+1}\|^2 - \|\delta_{x\bar{x}}^{(2)} e^{n-1}\|^2\big) \\ &\quad + \|\delta_x\bar{e}^n\|^2 + \frac{h^2}{12}\|\delta_{x\bar{x}}^{(2)}\bar{e}^n\|^2 + \langle\mathcal{A}_t\delta_{\hat{x}}e^n, 2\bar{e}^n\rangle + \frac{\gamma}{2}\langle\mathcal{A}_t\delta_{\hat{x}}\big[(v^n)^2 - (u^n)^2\big], 2\bar{e}^n\rangle \\ &= \langle r^n, \bar{e}^n\rangle, \end{aligned} \tag{28}$$

where $s_1$ is defined in Theorem 8. By Lemma 1, the Cauchy–Schwarz inequality, and Theorem 8, we see that

$$\begin{aligned} \langle\mathcal{A}_t\delta_{\hat{x}}e^n, 2\bar{e}^n\rangle &= \langle\delta_{\hat{x}}e^n, 2\bar{u}^n\rangle + \frac{\tau^2}{6}\langle\delta_{t\bar{t}}^{(2)}\delta_{\hat{x}}e^n, 2\bar{e}^n\rangle \\ &\le \|\delta_{\hat{x}}e^n\|^2 + \|\bar{e}^n\|^2 + \frac{1}{6}\big(\|\delta_{\hat{x}}e^{n+1}\|^2 + 2\|\delta_{\hat{x}}e^n\|^2 + \|\delta_{\hat{x}}e^{n-1}\|^2 + 3\|\bar{e}^n\|^2\big) \\ &\le \frac{1}{6}\|\delta_x e^{n+1}\|^2 + \frac{4}{3}\|\delta_x e^n\|^2 + \frac{1}{6}\|\delta_x e^{n-1}\|^2 + \frac{3}{4}\|e^{n-1}\|^2 + \frac{3}{4}\|e^{n+1}\|^2. \end{aligned} \tag{29}$$

Next, the nonlinear term can be estimated by applying Theorem 8, the Cauchy–Schwarz inequality, and the boundary conditions:

$$\begin{aligned} &\langle\mathcal{A}_t\delta_{\hat{x}}\big[(v^n)^2 - (u^n)^2\big], 2\bar{e}^n\rangle \\ &= \langle\delta_{\hat{x}}\big[(v^n)^2 - (u^n)^2\big], 2\bar{e}^n\rangle + \frac{\tau^2}{6}\langle\delta_{t\bar{t}}^{(2)}\delta_{\hat{x}}\big[(v^n)^2 - (u^n)^2\big], 2\bar{e}^n\rangle \\ &= -\langle\big[(v^n)^2 - (u^n)^2\big], 2\delta_{\hat{x}}\bar{e}^n\rangle - \frac{\tau^2}{6}\langle\delta_{t\bar{t}}^{(2)}\big[(v^n)^2 - (u^n)^2\big], 2\delta_{\hat{x}}\bar{e}^n\rangle \\ &= -\langle e^n(v^n + u^n), 2\delta_{\hat{x}}\bar{e}^n\rangle - \frac{\tau^2}{6}\langle\delta_{t\bar{t}}^{(2)}\big[e^n(v^n + u^n)\big], 2\delta_{\hat{x}}\bar{e}^n\rangle \\ &= -2h\sum_{i=1}^{M-1} e_i^n(v_i^n + u_i^n)\delta_{\hat{x}}(\bar{e}_i^n) - \frac{1}{3}\sum_{i=1}^{M-1} e_i^{n+1}(v_i^{n+1} + u_i^{n+1})\delta_{\hat{x}}(\bar{e}_i^n) \end{aligned}$$

$$+\frac{2}{3}\sum_{i=1}^{M-1} e_i^n\big(v_i^n+u_i^n\big)\delta_{\hat{x}}\big(\bar{e}_i^n\big)-\frac{1}{3}\sum_{i=1}^{M-1} e_i^{n-1}\big(v_i^{n-1}+u_i^{n-1}\big)\delta_{\hat{x}}\big(\bar{e}_i^n\big)$$
$$\leq C\big(\|e^{n-1}\|^2+\|e^n\|^2+\|e^{n+1}\|^2+\|\delta_x e^{n-1}\|^2+\|\delta_x e^{n+1}\|^2\big). \tag{30}$$

Furthermore,

$$\langle r^n,\bar{e}^n\rangle \leq \frac{1}{2}\|r^n\|^2+\frac{1}{4}\big(\|e^{n-1}\|^2+\|e^{n+1}\|^2\big). \tag{31}$$

Applying equations (29)–(31) with equation (28), we have

$$\big(\|e^{n+1}\|^2-\|e^{n-1}\|^2\big)+s_1\big(\|\delta_x e^{n+1}\|^2-\|\delta_x e^{n-1}\|^2\big)-\frac{\mu h^2}{12}\big(\|\delta_{x\bar{x}}^{(2)}e^{n+1}\|^2-\|\delta_{x\bar{x}}^{(2)}e^{n-1}\|^2\big)$$
$$\leq \tau\|r^n\|^2+\tau C\big(\|e^{n-1}\|^2+\|e^n\|^2+\|e^{n+1}\|^2+\|\delta_x e^{n-1}\|^2+\|\delta_x e^n\|^2+\|\delta_x e^{n+1}\|^2\big). \tag{32}$$

If $h$ is sufficiently small such that $4\mu-h^2>0$, by Lemma 4 and equation (32) can be estimated as follows:

$$\big(\|e^{n+1}\|^2-\|e^{n-1}\|^2\big)+\big(\|\delta_x e^{n+1}\|^2-\|\delta_x e^{n-1}\|^2\big)$$
$$\leq \tau\|r^n\|^2+\tau C\big(\|e^{n-1}\|^2+\|e^n\|^2+\|e^{n+1}\|^2+\|\delta_x e^{n-1}\|^2+\|\delta_x e^n\|^2+\|\delta_x e^{n+1}\|^2\big). \tag{33}$$

Let

$$\mathrm{Error}^n=\big(\|e^n\|^2+\|e^{n-1}\|^2\big)+s_1\big(\|\delta_x e_x^n\|^2+\|\delta_x e^{n-1}\|^2\big)+\frac{\mu h^2}{12}\big(\|\delta_{x\bar{x}}^{(2)}e^n\|^2+\|\delta_{x\bar{x}}^{(2)}e_x^{n-1}\|^2\big).$$

Then equation (33) can be rewritten as

$$\mathrm{Error}^{n+1}-\mathrm{Error}^n\leq 2\tau\|r^n\|^2+\tau C\big(\mathrm{Error}^{n+1}+\mathrm{Error}^n\big), \tag{34}$$

or, equivalently,

$$(1-\tau C)\big(\mathrm{Error}^{n+1}-\mathrm{Error}^n\big)\leq 2\tau\|r^n\|^2+2\tau C\mathrm{Error}^n.$$

If $\tau$ is sufficiently small such that $1-C\tau>0$, then

$$\mathrm{Error}^{n+1}-\mathrm{Error}^n\leq 2\tau\|r^n\|^2+2\tau C\mathrm{Error}^n. \tag{35}$$

Summing equation (35) from 1 to $n$, we have

$$\mathrm{Error}^{n+1}-\mathrm{Error}^1\leq 2\tau\sum_{k=2}^{n}\|r^k\|^2+\tau C\sum_{k=1}^{n}\mathrm{Error}^k\leq C\big(\tau^2+h^4\big)^2+\tau C\sum_{k=1}^{n}\mathrm{Error}^k, \tag{36}$$

where we used

$$2\tau\sum_{k=2}^{n}\|r^k\|^2\leq 2(n-1)\tau\max_{2\leq k\leq n}\|r^k\|^2\leq C\big(\tau^2+h^4\big)^2.$$

Since we can approximate $u^1$ using any available fourth-order accuracy method, we have $\text{Error}^1 = \mathcal{O}(\tau^2 + h^4)^2$. Hence by Lemma 6 we obtain

$$\text{Error}^{n+1} \leq \mathcal{O}\big(\tau^2 + h^4\big)^2,$$

that is,

$$\big\|e^{n+1}\big\|^2 \leq \mathcal{O}\big(\tau^2 + h^4\big)^2 \quad \text{and} \quad \big\|e_x^{n+1}\big\|^2 \leq \mathcal{O}\big(\tau^2 + h^4\big)^2.$$

Finally, by Lemma 5 we get

$$\big\|e^{n+1}\big\|_\infty^2 \leq \mathcal{O}\big(\tau^2 + h^4\big)^2.$$

To complete the proof when $\alpha = 0$, note that $\|e^{n+1}\|_\infty^2 \leq \mathcal{O}(\tau^4 + h^4)^2$ by applying a similar technique. □

**Theorem 13** *Under the conditions of Theorem 12, the solution of scheme (8)–(10) is stable in the sense of $\|\cdot\|_\infty$-norm.*

Since the proposed scheme is a nonlinear implicit FDS, to solve the scheme, we provide an iterative algorithm. The strategy is not uncommon in solving this kind of nonlinear schemes. Applying the techniques of Sun and Zhu [41] (see also [42]), we then obtain an iterative algorithm to solve the nonlinear term for $s = 0, 1, 2, \ldots$. We observe that scheme (8)–(10) can be solved as follows:

$$\begin{aligned} &\mathcal{A}_x\big(u_i^{(n+1)(s+1)} - u_i^{n-1}\big) - \mu\mathcal{A}_x\delta_{x\bar{x}}^{(2)}\big(u_i^{(n+1)(s+1)} - u_i^{n-1}\big) + \mu\frac{h^2}{12}\delta_{xx\bar{x}\bar{x}}^{(4)}\big(u_i^{(n+1)(s+1)} - u_i^{n-1}\big) \\ &\quad - \tau\alpha\mathcal{L}_x\delta_{x\bar{x}}^{(2)}\big(u_i^{(n+1)(s+1)} + u_i^{n-1}\big) + 2\tau\delta_{\hat{x}}\big(u^n\big) + \frac{\tau}{3}\big(u_i^{(n+1)(s+1)} - 2u_i^n + u_i^{n-1}\big) \\ &\quad + \tau\gamma\delta_{\hat{x}}\big[\big(u_i^n\big)^2\big] + \gamma\frac{\tau}{6}\delta_{\hat{x}}\big[\big(u_i^{(n+1)(s)}\big)^2 - 2\big(u_i^n\big)^2 + \big(u_i^{n-1}\big)^2\big], \end{aligned} \tag{37}$$

where $u_i^{(n+1)(0)} = 2u_i^n - u_i^{n-1}$ with the initial condition

$$u_i^0 = u_0(x_i), \quad 0 \leq i \leq M, \tag{38}$$

and the boundary conditions

$$u_0^n = u_M^n = 0, \qquad \delta_{\hat{x}}\big(u_0^n\big) = \delta_{\hat{x}}\big(u_M^n\big) = 0, \qquad \delta_{x\bar{x}}^{(2)}\big(u_0^n\big) = \delta_{x\bar{x}}^{(2)}\big(u_M^n\big) = 0, \quad 1 \leq n \leq N. \tag{39}$$

Algorithm (37) can be written as

$$\begin{aligned} &\mathcal{A}_x\big(u_i^{(n+1)(s+1)}\big) - \mu\mathcal{A}_x\delta_{x\bar{x}}^{(2)}\big(u_i^{(n+1)(s+1)}\big) + \mu\frac{h^2}{12}\delta_{xx\bar{x}\bar{x}}^{(4)}\big(u_i^{(n+1)(s+1)}\big) \\ &\quad - \tau\alpha\mathcal{L}_x\delta_{x\bar{x}}^{(2)}\big(u_i^{(n+1)(s+1)}\big) + \frac{\tau}{3}\big(u_i^{(n+1)(s+1)}\big) = b_i^{(n)(s)}, \end{aligned}$$

where

$$b_i^{(n)(s)} = \mathcal{A}_x\big(u_i^{n-1}\big) + \mu\mathcal{A}_x\delta_{x\bar{x}}^{(2)}\big(u_i^{n-1}\big) + \mu\frac{h^2}{12}\delta_{xx\bar{x}\bar{x}}^{(4)}\big(u_i^{n-1}\big) + \tau\alpha\mathcal{L}_x\delta_{x\bar{x}}^{(2)}\big(u_i^{n-1}\big) - 2\tau\delta_{\hat{x}}\big(u^n\big)$$

$$+\frac{\tau}{3}\left(2u_i^n-u_i^{n-1}\right)-\tau\gamma\delta_{\hat{x}}\left[\left(u_i^n\right)^2\right]$$
$$-\tau\gamma\delta_{\hat{x}}\left[\left(u_i^n\right)^2\right]+\gamma\frac{\tau}{6}\delta_{\hat{x}}\left[\left(u_i^{(n+1)(s)}\right)^2-2\left(u_i^n\right)^2+\left(u_i^{n-1}\right)^2\right]. \qquad (40)$$

Here we provide an algorithm for solving scheme (8)–(10):

**Algorithm**

*step 1* Let $u_i^{(n+1)(0)}=2u_i^n-u_i^{n-1}$.

*step 2* Compute $u_i^{(n+1)(s+1)}$ iteratively solving the equation

$$\mathbf{P}\mathbf{u}^{(n+1)(s+1)}=\mathbf{b}^{(n)(s)},\quad s=0,1,2,\dots,$$

where

$$\mathbf{P}=\begin{bmatrix} k_3 & k_2 & k_1 & 0 & \cdots & 0 & 0\\ k_2 & k_3 & k_2 & k_1 & \ddots & \vdots & 0\\ k_1 & k_2 & k_3 & k_2 & k_1 & \vdots & \vdots\\ \vdots & \ddots & \ddots & \ddots & \ddots & \ddots & 0\\ \vdots & \ddots & k_1 & k_2 & k_3 & k_2 & k_1\\ 0 & 0 & \cdots & k_1 & k_2 & k_3 & k_2\\ 0 & 0 & \cdots & 0 & k_1 & k_2 & k_3 \end{bmatrix},$$

$$\mathbf{u}^{(n+1)(s+1)}=\begin{bmatrix} u_1^{(n+1)(s+1)}\\ u_2^{(n+1)(s+1)}\\ \vdots\\ \vdots\\ u_{M-1}^{(n+1)(s+1)} \end{bmatrix},\quad \text{and}\quad \mathbf{b}^{(n)(s)}=\begin{bmatrix} b_1^{(n)(s)}\\ b_2^{(n)(s)}\\ \vdots\\ \vdots\\ b_{M-1}^{(n)(s)} \end{bmatrix}$$

with

$$k_1=-\frac{\mu+\tau\alpha}{12h^2},\qquad k_2=\frac{1}{6}-\frac{2(\mu+2\tau\alpha)}{3h^2},\qquad \text{and}\quad k_3=\frac{2}{3}+\frac{\tau}{3}+\frac{3\mu+5\tau\alpha}{2h^2}.$$

The iterations will be done when the approximate solution satisfies the criterion

$$\left\|u^{(n+1)(s+1)}-u^{(n+1)(s)}\right\|_\infty\le 10^{-10}.$$

The additional advantage of using this algorithm is that it results in iteratively solving the constant coefficient pentadiagonal system at each time step, which expectedly saves the computation time. Before proving the convergence of the iterative algorithm, we let

$$\varepsilon_i^{(s)}=u_i^{(n+1)(s)}-u_i^{n+1}.$$

Note that

$$\varepsilon_i^{(0)}=u_i^{n+1}-2u_i^n+u_i^{n-1}$$
$$\le\left(u_i^{n+1}-v_i^{n+1}\right)-2\left(u_i^n-v_i^n\right)+\left(u_i^{n-1}-v_i^{n-1}\right)+v_i^{n+1}-2v_i^n+v_i^{n-1}$$

$$\le O(\tau^2 + h^4).$$

Similarly, we also have

$$\left(\varepsilon_i^{(0)}\right)_x \le O(\tau^2 + h^4), \qquad \left(\varepsilon_i^{(0)}\right)_{xx} \le O(\tau^2 + h^4).$$

**Theorem 14** *Let $\tau$ and $h$ be sufficiently small. Then the iterative algorithm* (37)–(39) *converges to the solution of scheme* (8)–(10).

*Proof* Letting $\tau$ and $h$ be sufficiently small, we have

$$\left\|\varepsilon^{(0)}\right\|_\infty \le \frac{1}{2}.$$

Suppose

$$\left\|\varepsilon^{(s)}\right\|_\infty \le \frac{1}{2}. \tag{41}$$

By Theorem 8 and assumption (41) we see that

$$\left\|u^{(n+1)(s)}\right\|_\infty \le \left\|u^{n+1}\right\|_\infty + \left\|\varepsilon^{(s)}\right\|_\infty \le C.$$

Subtracting equation (37) from equation (8), we have

$$\begin{aligned} &\mathcal{A}_x\left(\varepsilon_i^{(s+1)}\right) - \mu\mathcal{A}_x\delta_{x\bar{x}}^{(2)}\left(\varepsilon_i^{(s+1)}\right) + \mu\frac{h^2}{12}\delta_{xx\bar{x}\bar{x}}^{(4)}\left(\varepsilon_i^{(s+1)}\right) \\ &\quad - \tau\alpha\mathcal{L}_x\delta_{x\bar{x}}^{(2)}\left(\varepsilon_i^{(s+1)}\right) + \frac{\tau}{3}\left(\varepsilon_i^{(s+1)}\right) + \gamma\frac{\tau}{6}\delta_{\hat{x}}\left[\left(u_i^{(n+1)(s)}\right)^2 - \left(u_i^{n+1}\right)^2\right] = 0. \end{aligned} \tag{42}$$

Taking the inner product of (42) with $\varepsilon^{(s+1)}$, by Lemmas 1 and 2 we have

$$\begin{aligned} &\left\|\varepsilon^{(s+1)}\right\|^2 + s_4\left\|\delta_x\varepsilon^{(s+1)}\right\|^2 + \tau\alpha\frac{h^2}{12}\left\|\delta_{x\bar{x}}^{(2)}\varepsilon^{(s+1)}\right\|^2 \\ &\quad + \frac{\gamma\tau}{3}\left\langle\delta_{\hat{x}}\left[\left(u^{(n+1)(s)}\right)^2 - \left(u^{n+1}\right)^2\right], \varepsilon^{(s+1)}\right\rangle = 0, \end{aligned} \tag{43}$$

where $s_4$ is as defined in Theorem 11. Similarly to the technique used in equation (26), we have

$$\left\langle\delta_{\hat{x}}\left[\left(u^{(n+1)(s)}\right)^2 - \left(u^{n+1}\right)^2\right], \varepsilon^{(s+1)}\right\rangle \le C\left(\left\|\varepsilon^{(s)}\right\|^2 + \left\|\delta_x\varepsilon^{(s+1)}\right\|^2\right),$$

which yields

$$\left\|\varepsilon^{(s+1)}\right\|^2 + s_4\left\|\delta_x\varepsilon^{(s+1)}\right\|^2 + \tau\alpha\frac{h^2}{12}\left\|\delta_{x\bar{x}}^{(2)}\varepsilon^{(s+1)}\right\|^2 \le \tau C\left(\left\|\varepsilon^{(s)}\right\|^2 + \left\|\delta_x\varepsilon^{(s+1)}\right\|^2\right).$$

By Lemma 4 we can estimate this equation as follows:

$$\left\|\varepsilon^{(s+1)}\right\|^2 + (s_4 - \tau C)\left\|\delta_x\varepsilon^{(s+1)}\right\|^2 + \tau\alpha\frac{h^2}{12}\left\|\delta_{x\bar{x}}^{(2)}\varepsilon^{(s+1)}\right\|^2 \le \tau C\left\|\varepsilon^{(s)}\right\|^2.$$

Let $\tau$ be sufficiently small such that $s_4 - \tau C > 0$. By the positivity of the term $\tau\alpha\|\delta_{x\bar{x}}^{(2)}\varepsilon^{(s+1)}\|^2$ we get

$$\|\varepsilon^{(s+1)}\|^2 + \|\delta_x\varepsilon^{(s+1)}\|^2 \le \tau C\|\varepsilon^{(s)}\|^2 \le \tau C\|\varepsilon^{(s)}\|_\infty^2. \tag{44}$$

Again, let $\tau$ be sufficiently small such that $\tau C \le \frac{1}{2}$. By Lemma 5 we have

$$\|\varepsilon^{(s+1)}\|_\infty \le \frac{1}{2}\|\varepsilon^{(s)}\|_\infty \le \frac{1}{2^{s+1}}\|\varepsilon^{(0)}\|_\infty.$$

This completes the proof. □

The following theorem guarantees the mass-preserving property, which can be derived by using the same technique as in Theorem 7. So we omit the proof.

**Theorem 15** *Suppose $u^{(n+1)(s+1)} \in Z_{h,0}$. Then algorithm (37) is conservative in the sense that*

$$\begin{aligned} I_{1,1}^{n,(s+1)} &= \frac{h}{2}\sum_{i=1}^{M-1}\left(u_i^{(n+1)(s+1)} + u_i^n\right) \\ &= \frac{h}{2}\sum_{i=1}^{M-1}\left(u_i^{n+1} + u_i^n\right) \end{aligned}$$

*for all $s = 0, 1, 2, \ldots$.*

## 4 Numerical experiments

We will perform a few numerical experiments in this section to verify the effectiveness and correctness of our theoretical analysis from the preceding part using the evolution of the single solitary wave. The proposed scheme is referred to as Scheme I for convenience. Here we compare the accuracy of the proposed scheme to the error of the previous schemes to demonstrate its precision.

*Scheme II*: Fourth-order linear implicit FDS [30]

$$\begin{aligned} &\delta_{\hat{t}}\left(u_i^n\right) - \mu\left[\frac{4}{3}\delta_{\hat{t}}\delta_{x\bar{x}}^{(2)}\left(u_i^n\right) + \frac{1}{3}\delta_{\hat{t}}\delta_{\hat{x}\hat{x}}^{(2)}\left(u_i^n\right)\right] \\ &\quad + \frac{4}{3}\delta_{\hat{x}}\left(\bar{u}_i^n\right) - \frac{1}{3}\delta_{\ddot{x}}\left(\bar{u}_i^n\right) - \alpha\left[\frac{4}{3}\delta_{x\bar{x}}^{(2)}\left(\bar{u}_i^n\right) + \frac{1}{3}\delta_{\hat{x}\hat{x}}^{(2)}\left(\bar{u}_i^n\right)\right] \\ &\quad + \frac{\gamma}{3}\left[\frac{4}{3}u_i^n\delta_{\hat{x}}\left(\bar{u}_i^n\right) - \frac{1}{3}u_i^n\delta_{\ddot{x}}\left(\bar{u}_i^n\right)\right] + \frac{\gamma}{3}\left[\frac{4}{3}\delta_{\hat{x}}\left(u_i^n\bar{u}_i^n\right) - \frac{1}{3}\delta_{\ddot{x}}\left(u_i^n\bar{u}_i^n\right)\right] = 0, \end{aligned} \tag{45}$$

and a modified linear three-level FDS from the recently published paper [18]. We substitute the approximation of a dispersive term $u_{xxx}$ in [18] by an average approximation of the viscous term $\partial_x^2 u(x_i, t^n) = (\bar{u}_i^n)_{x\bar{x}} + \mathcal{O}(\tau^2 + h^2)$. The scheme turns into the following scheme.

*Scheme III*: Standard second-order linear implicit FDS

$$\delta_{\hat{t}}\left(u_i^n\right) - \mu\delta_{\hat{t}}\delta_{x\bar{x}}^{(2)}\left(u_i^n\right) + \delta_{\hat{x}}\left(\bar{u}_i^n\right) - \alpha\delta_{x\bar{x}}^{(2)}\left(\bar{u}_i^n\right) + \frac{\gamma}{3}\left[u_i^n\delta_{\hat{x}}\left(\bar{u}_i^n\right) + \delta_{\hat{x}}\left(u_i^n\bar{u}_i^n\right)\right] = 0. \tag{46}$$

We can easily see that the boundedness, stability, and convergence of scheme (46) can be studied by changing the arguments in [18] (see also [19]). We would like to notice that Scheme III is reliable due to the existing publications, that is, we obtain the FDS obtained by Zhang [19] for RLW equation (in the case $p = 2$ and $\theta = 0$), where $\theta$ is a parameter appearing in the mentioned schemes.

*Remark* 16 In Schemes II and III the difference approximation of the nonlinear term $uu_x$ is widely used to ensure the energy conservation, stability, and convergence of the numerical solutions. For further information, the reader should consult references [43–47] for various types of equations with the same treatments of the nonlinear term $uu_x$.

The precision of the method is determined by comparing numerical solutions to exact solutions using the $\|\cdot\|$- and $\|\cdot\|_\infty$-norms represented by

$$\|e^n\| = \|u^{\text{exact}} - u^n\| = \left(h\sum_{i=1}^{M-1}\left|u(x_i,t^n) - u_i^n\right|^2\right)^{\frac{1}{2}},$$
$$\|e^n\|_\infty = \|u^{\text{exact}} - u^n\|_\infty = \max_i\left|u(x_i,t^n) - u_i^n\right|,$$

respectively. We design the numerical comparisons in two aspects. In the first example, we provide the numerical simulations for the solution of the RLW equation in the case of $\alpha = 0$. From the theoretical expectation the fourth-order convergence rate is monitored via the exact solitary waveform when $\tau = h$. Another example is the BBM–Burgers equation. The nonhomogeneous case is used to test the convergence rate to ensure Theorem 12, where the time and space discretization are chosen to be $\tau = h^2$. The long-time simulations and computational time in both examples are also observed. We anticipate that its computational cost scales should be less than the others.

*Example* 1 The RLW equation: The single solitary wave.

In the first example, we consider the following RLW equation ($\mu = 1$, $\alpha = 0$, $\gamma = 1$)

$$u_t - u_{xxt} + u_x + uu_x = 0, \tag{47}$$

which has an analytic solution of the form

$$u(x,t) = 3c\,\text{sech}^2\big(m\big(x - (c+1)t - x_0\big)\big), \tag{48}$$

where $m = \frac{1}{2}\sqrt{\frac{c}{1+c}}$. The solution stands for a single solitary wave having the amplitude $3c$ centered at $x_0$ with the velocity $v = 1 + c$. Thus the initial and boundary conditions corresponding to the exact solution are given for equation (47) as follows:

$$u(x,0) = 3c\,\text{sech}^2\big[m(x - x_0)\big], \tag{49}$$

and

$$u_0^n = u_M^n = 0, \qquad \delta_{\hat{x}}\big(u_0^n\big) = \delta_{\hat{x}}\big(u_M^n\big) = 0, \qquad \delta_{x\bar{x}}^{(2)}\big(u_0^n\big) = \delta_{x\bar{x}}^{(2)}\big(u_M^n\big) = 0, \quad 1 \le n \le N. \tag{50}$$

**Table 1** The errors of numerical solutions and rate of convergence at $T = 20$ using $h = \tau$

| | $\tau = h$ | $\|\cdot\|$ | Rate | $\|\cdot\|_\infty$ | Rate | CPU time (s) |
|---|---|---|---|---|---|---|
| Scheme I | 0.5 | $5.4875 \times 10^{-6}$ | – | $2.2094 \times 10^{-6}$ | – | 0.0857 |
| | 0.25 | $3.3976 \times 10^{-7}$ | 4.0136 | $1.3672 \times 10^{-7}$ | 4.0144 | 0.3099 |
| | 0.125 | $2.1207 \times 10^{-8}$ | 4.0019 | $8.5434 \times 10^{-9}$ | 4.0003 | 1.0363 |
| | 0.0625 | $1.3250 \times 10^{-9}$ | 4.0004 | $5.3515 \times 10^{-10}$ | 3.9968 | 8.8850 |
| Scheme II [30] | 0.5 | $1.8618 \times 10^{-2}$ | – | $7.0602 \times 10^{-3}$ | – | 0.0813 |
| | 0.25 | $4.7664 \times 10^{-3}$ | 1.9657 | $1.8134 \times 10^{-3}$ | 1.9610 | 0.4885 |
| | 0.125 | $1.1996 \times 10^{-3}$ | 1.9903 | $4.5739 \times 10^{-4}$ | 1.9872 | 5.5283 |
| | 0.0625 | $3.0053 \times 10^{-4}$ | 1.9970 | $1.1465 \times 10^{-4}$ | 1.9962 | 47.0629 |
| Scheme III [18, 19] | 0.5 | $1.4946 \times 10^{-3}$ | – | $5.2670 \times 10^{-4}$ | – | 0.0591 |
| | 0.25 | $1.3373 \times 10^{-4}$ | 1.9808 | $5.1894 \times 10^{-4}$ | 1.9777 | 0.3434 |
| | 0.125 | $9.5127 \times 10^{-5}$ | 1.9930 | $3.3644 \times 10^{-5}$ | 1.9909 | 2.4583 |
| | 0.0625 | $2.3828 \times 10^{-5}$ | 1.9972 | $8.4277 \times 10^{-6}$ | 1.9971 | 22.0431 |

Scheme II is exactly the same scheme with those in [18, 19] in the case of RLW equation when the parameter $\theta$ in [19] is chosen to be 0.

In the simulation the present scheme is tested numerically for the cases $c = 0.1$ with $x_0 = 0$ over the space interval $[-80, 100]$ and time interval $[0, 20]$. The average and maximal errors under different step sizes $\tau$ and $h$ at the final time $T = 20$ are reported in Table 1. We see that the proposed scheme outperforms comparable Schemes II and III. The error obtained over a wide step size $h = \tau = 0.5$ by Scheme I is still more accurate than that obtained by Scheme II over a narrower step size $h = \tau = 0.0625$. In addition, as we intended, the computational efficiency of the present scheme is outstanding compared to Schemes II and III in terms of CPU time due to the requirement of solving the system of equation in each time step. Besides, as shown in the table, the rate of convergence is close to the theoretical expectations for each scheme. The fourth-order convergence can be achieved by Scheme I as we expected, whereas the accuracy of Schemes II and III is found to be of second order. Here we note that the second-order convergence of Scheme II is commonplace because the accuracy in space is absorbed by the error in time ($\tau = h$).

Next, we provide a numerical solution at long-time behavior and make simulations at $T = 500$ over the computational domain $[-100, 700]$ with $c = 0.1$ under setting the rough space and time step sizes $h = \tau = 0.5$. Figure 1 shows the profiles of the numerical solutions of Schemes I, II, and III. Figure 1 (top) shows the accuracy of Schemes I and II while lagging of the numerical solution of Scheme III is clearly observed. Moreover, in Fig. 1 (bottom), the small wave trains and visible oscillations of the numerical solutions occur when Schemes III and III are applied, respectively, whereas the presented scheme provides almost an identical solution on the left tail. Figure 2 indicates that the presented scheme successfully provides approximate solutions in computation and is obviously more accurate than the schemes in [18, 19] and [30] with the same step sizes during the time from $T = 0$ to $T = 500$. Observe that the error slightly increases almost linearly as time increases in both error norms. The $\|\cdot\|$- and $\|\cdot\|_\infty$-norms of te errors of the proposed scheme stay less than $8.7 \times 10^{-4}$ over time up to $T = 500$, which produces very good satisfactory results compared to Schemes II and III.

The process is reproduced in 10-fold simulations to gather the computational costs. The results are shown in Fig. 3. The expense of computational cost of Schemes II and III are approximately two and four orders of magnitude greater. Accordingly, it is clear that the trade-off between solving the nonlinear scheme and computational cost is apparently relieved.

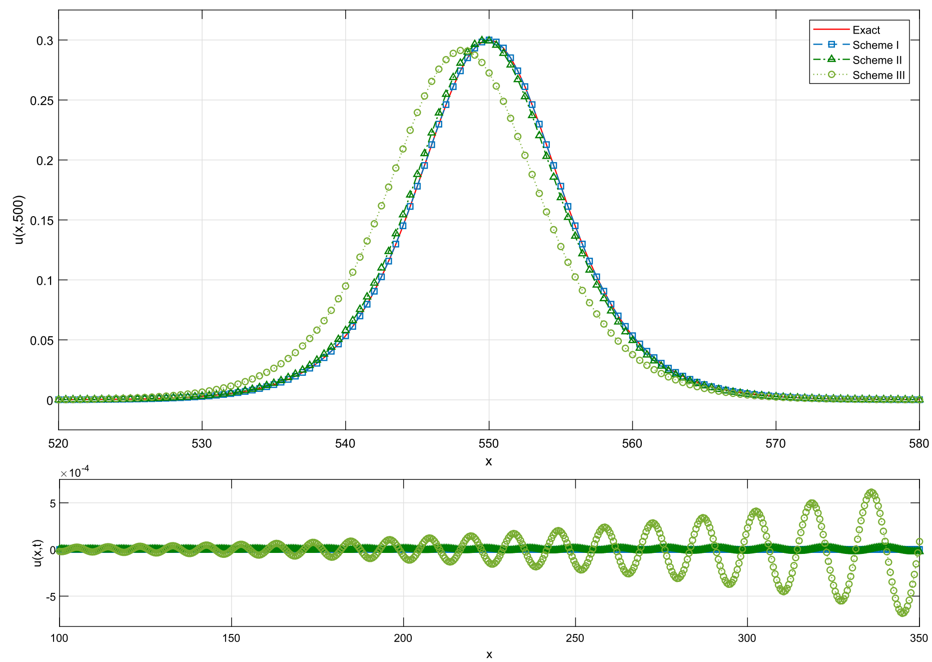


**Figure 1** The long-time behavior of numerical solutions at $T = 500$ using $h = \tau = 0.5$

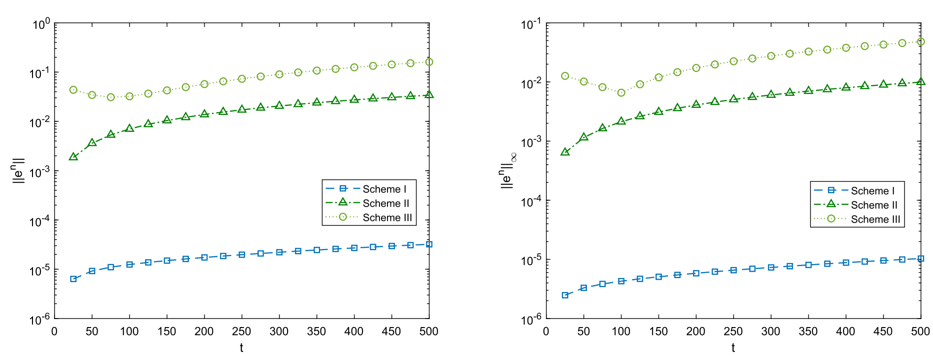


**Figure 2** Evolution of $\|\cdot\|$-error (left) and $\|\cdot\|_\infty$-error (right) until $T = 500$ using $h = \tau = 0.5$

As an indication of the efficiency of the numerical method, there is not only the order of accuracy, but also other essential factors, especially the invariant-preserving property. To examine the conservation properties of our scheme, we provide the absolute error of these invariants for the RLW equation as the following discretization:

$$I_1^n = \int_a^b u(x,t^n)\,dx \approx h\sum_{i=1}^{M-1} u_i^n, \tag{51}$$

$$I_2^n = \int_a^b \left(u^2(x,t^n) + u_x^2(x,t^n)\right)dx \approx h\sum_{i=1}^{M-1}\left(\left(u_i^n\right)^2 + \left[\left(u_i^n\right)_{\hat{x}}\right]^2\right), \tag{52}$$

$$I_3^n = \int_a^b \left(u^3(x,t^n) + 3u^2(x,t^n)\right)dx \approx h\sum_{i=1}^{M-1}\left(\left(u_i^n\right)^3 + 3\left(u_i^n\right)^2\right). \tag{53}$$

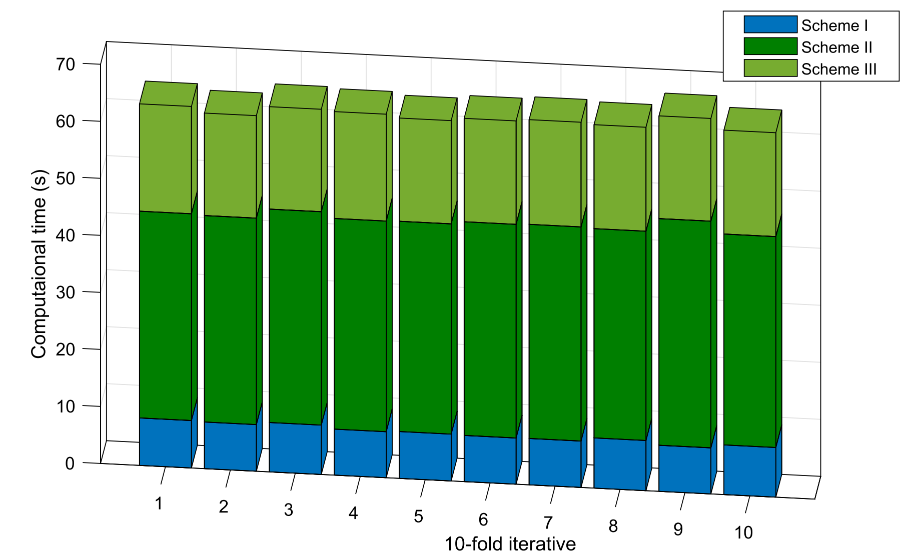


**Figure 3** Computational time (s) in each fold

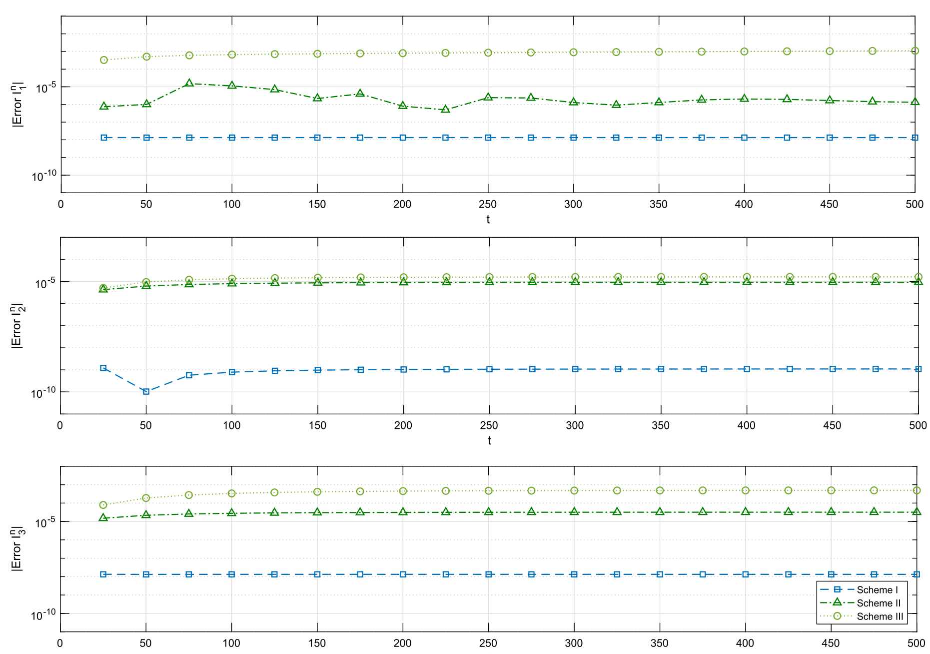


**Figure 4** Error of invariant properties

For Scheme I, the formula of the quality $I_1^n$ follows from Theorem 7 (see also Theorem 15), whereas the invariants $I_2^n$ and $I_3^n$ can be approximately achieved by equations (52) and (53), respectively. Likewise, we evaluate the qualities $I_1^n$, $I_2^n$, and $I_3^n$ for Schemes II and III by equations (51)–(53). The changing of invariants is shown in Fig. 4. We are able to detect that the quantities $I_1^n$, $I_2^n$, and $I_3^n$ are considerably preserved during $T = 0$ to $T = 500$. The conservative property of the presented scheme is perfectly preserved at least 7 digits and more accurate compared with Schemes II and III.

**Table 2** A comparison of accuracy between the present scheme and the other methods when $h = 0.125$ and $\tau = 0.1$ at $T = 20$

| | $\|\cdot\| \times 10^4$ | $\|\cdot\|_\infty \times 10^4$ |
|---|---|---|
| Scheme I | $2.99 \times 10^{-4}$ | $1.20 \times 10^{-4}$ |
| Scheme II [18, 19, 29] | 12.973 | 4.9672 |
| Scheme III [30] | 7.6865 | 2.9312 |
| Splitting method and cubic spline [10] | 1961 | 67.4 |
| Least-squares FES [11] | 46.9 | 17.6 |
| Bubnov–Galerkin method [12] | 5.15 | 1.81 |
| Linear Galerkin method [13] | 5.11 | 1.98 |
| Collocation method [14] | 5.32 | 2.27 |
| Lumped Galerkin method [15] | 2.19 | 0.86 |
| Galerkin method with extrapolation [16] | 2.67 | 0.91 |
| Local conservative schemes [17] | | |
| ILMP-I | 0.15 | 0.05 |
| ILMP-II | 7.45 | 2.87 |
| ELMP-I | 6.66 | 2.58 |
| ELMP-II | 0.86 | 0.28 |
| Galerkin method with cubic B-splines ($h = 0.1$) [36] | 2.16 | 0.84 |

To clarify the efficiency of our scheme, we make numerical comparisons with existing methods, not limited to FDM [10–19, 36]. To set up the comparison, the velocity is set to be $v = 1.1$, that is, $c = 0.1$. The step sizes are chosen as $h = 0.125$ and $\tau = 0.1$, and the final time $T = 20$. The simulations are computed for the region $[-80, 100]$ to make sure the pulse is sufficiently small, corresponding to the boundary conditions. Table 2 shows the errors of the presented method and some recorded results obtained by the mentioned methods. As shown in the table, the error obtained by the proposed scheme is excellently better than those of the others. This significantly confirms that the results obtained by our scheme show an improvement over the other methods with a simplified FDM.

*Example* 2 The BBM–Burgers equation and the effect of viscous term to the RLW equation.

In this example, we consider the following BBM–Burgers equation ($\mu = 1$ and $\gamma = 1$):

$$u_t - u_{xxt} + u_x - \alpha u_{xx} + uu_x = f(x,t) \tag{54}$$

with the initial condition (49) and boundary conditions (50). Firstly, we set the nonhomogeneous function $f$ in compliance with the exact solution (48) when $c = 0.1$ to verify the order of accuracy and the rate of convergence. The simulations are also computed by the mentioned schemes in the case $\alpha = 1$ at the final time $T = 20$ over the computational domain $[-80, 100]$. The spatial and temporal step sizes are selected by $\tau = h^2$ to show the precision in time and space so that the dominant error is not based on only one aspect. The comparisons are made and listed in Table 3. The results show that the accuracy of Scheme I is slightly better than that of Scheme II at least by 59.06% improvement. However, the errors obtained by Schemes I and II show the advancement in accuracy compared with Scheme III. The convergence rates are close to theoretical expectations of each scheme; that is, the fourth-order rate of convergence is observed by Schemes I and II, whereas the second-order rate of convergence is observed for Scheme III as anticipated.

Suggested by the numerical experiments, it is evident that the proposed scheme is effective and robust in solving both the RLW and BBM-Burgers equations in terms of ac-

**Table 3** The errors of numerical solutions and rate of convergence for the BBM–Burgers equation (54) at $T = 20$ using $\tau = h^2$

| | $h$ | $\|\cdot\|$ | Rate | $\|\cdot\|_\infty$ | Rate | CPU time (s) |
|---|---|---|---|---|---|---|
| Scheme I | 0.5 | $9.4642 \times 10^{-4}$ | – | $4.0490 \times 10^{-4}$ | – | 0.1944 |
| | 0.25 | $5.8886 \times 10^{-5}$ | 4.0065 | $2.5164 \times 10^{-5}$ | 4.0081 | 1.1024 |
| | 0.125 | $3.6789 \times 10^{-6}$ | 4.0006 | $1.5740 \times 10^{-6}$ | 3.9989 | 8.2897 |
| | 0.0625 | $2.2991 \times 10^{-7}$ | 4.0001 | $9.8361 \times 10^{-8}$ | 4.0002 | 103.6436 |
| Scheme II [30] | 0.5 | $2.3023 \times 10^{-3}$ | – | $8.1853 \times 10^{-4}$ | – | 0.1838 |
| | 0.25 | $1.4378 \times 10^{-4}$ | 4.0012 | $5.1110 \times 10^{-5}$ | 4.0013 | 2.0441 |
| | 0.125 | $8.9858 \times 10^{-6}$ | 4.0000 | $3.1958 \times 10^{-6}$ | 3.9994 | 41.0603 |
| | 0.0625 | $5.6162 \times 10^{-7}$ | 4.0000 | $1.9970 \times 10^{-7}$ | 4.0003 | 837.0102 |
| Scheme III | 0.5 | $5.8714 \times 10^{-3}$ | – | $2.0247 \times 10^{-3}$ | – | 0.1222 |
| | 0.25 | $1.0506 \times 10^{-3}$ | 2.4825 | $3.6048 \times 10^{-4}$ | 2.4897 | 1.4217 |
| | 0.125 | $2.3683 \times 10^{-4}$ | 2.1493 | $8.1093 \times 10^{-5}$ | 2.1523 | 20.3022 |
| | 0.0625 | $5.7601 \times 10^{-5}$ | 2.0397 | $1.9710 \times 10^{-5}$ | 2.0407 | 360.4731 |

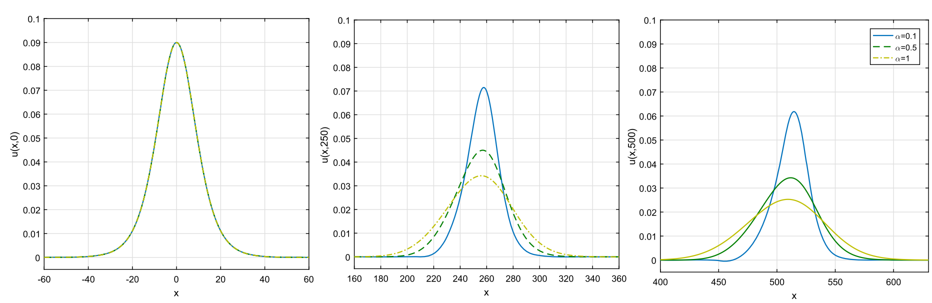


**Figure 5** Numerical solutions with $h = \tau = 0.5$ with different $\alpha = 0.1, 0.5$, and 1 at selected times $T = 0, 250$, and 500

curacy, computational cost, and conservation of fundamental qualities. Based on this approach, we further explore the effect of the linear viscous term on the RLW model related to a classical initial condition (49) with various velocity $c$. In the simulations the step sizes are chosen as $h = 0.5$ and $\tau = 0.25$, and the computational region is extended to $[-100, 700]$. Firstly, we let $c = 0.03$ and study the effect of the parameter $\alpha$ on the behavior of numerical solutions at time up to $T = 500$. Figure 5 shows the snapshots of the numerical solutions with different values of $\alpha = 0.1, 0.5$, and 1. The numerical simulations show that the parameter $\alpha$ affects the amplitudes of the numerical solutions but not the speed. It indicates that the numerical solution moves to the right in the same way as the analytic solution (48). Additionally, by observation the maximum of numerical solutions decreases as $\alpha$ increases. Evidently, the amplitude of $u(x,t)$ also decrease as time decreases.

Next, we study the relations between the parameter $\alpha$ and the initial velocity by setting the different parameters $c$. Let $c = 0.03, 0.1$, and 0.2 with different $\alpha = 0.1, 0.5$, and 1. The different values of $c$ and $\alpha$ provide similar propagations and disintegrations of the numerical solution as presented in Fig. 6. As time passes, the amplitude of the wave decreases, whereas the wave width grows. It should be pointed out by this observation that the obtained numerical solutions converge to 0 as time increases in the case of $\alpha \neq 0$. Actually, the behavior is supported by the theoretical results of the large-time behavior of the solu-

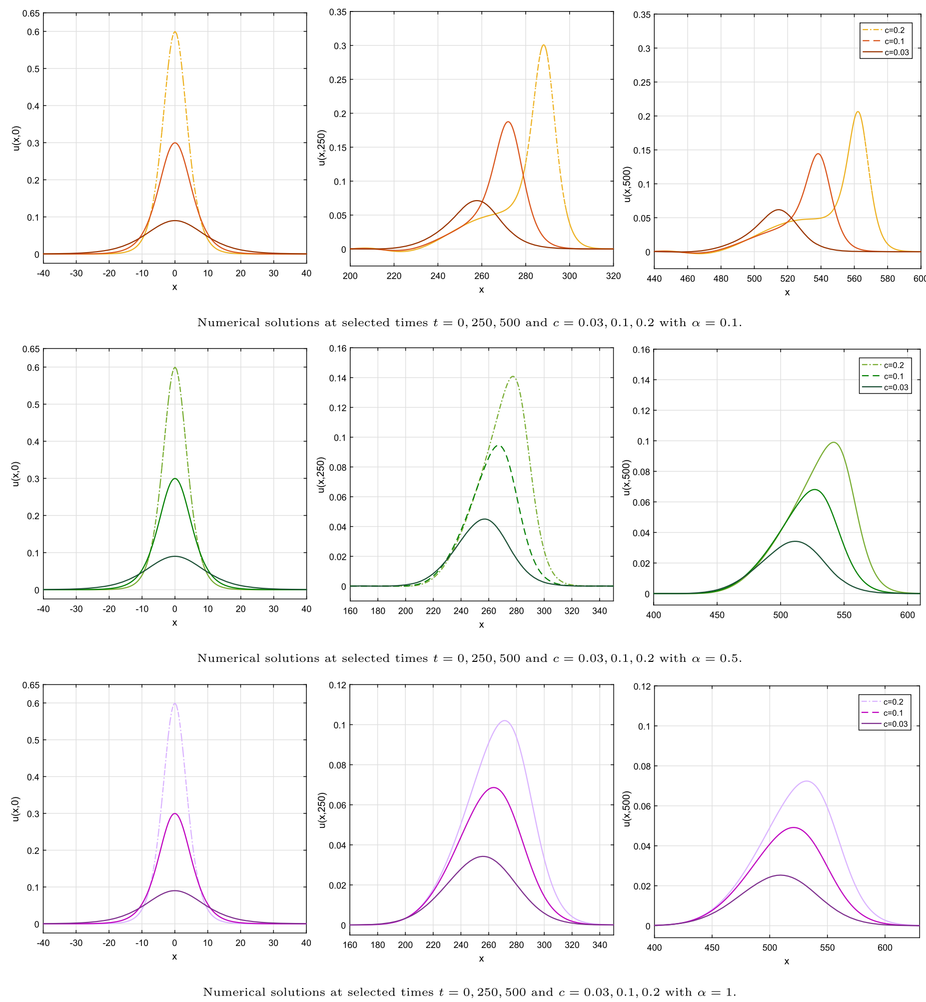


**Figure 6** Profile of numerical solutions with different $c$ and $\boldsymbol{\alpha}$ at selected times $T = 0$, 250, and 500

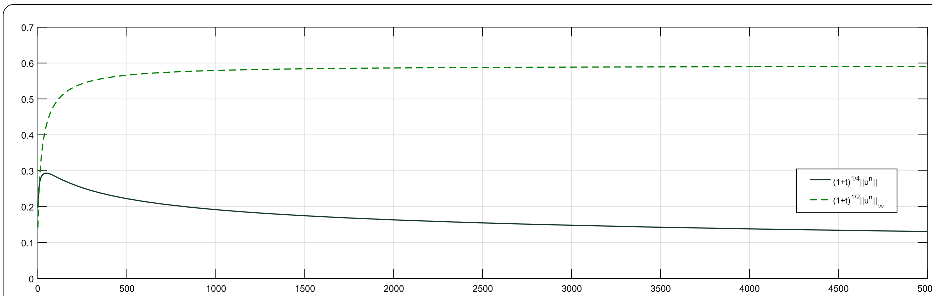


**Figure 7** The ratio rate corresponding to the initial condition (49)

tion for the Cauchy problem (54) in [48, 49]. The discussion results in [50] give

$$\left\|u(x,t)\right\|_{L_2} \leq C(1+t)^{-1/4}, \qquad \left\|u(x,t)\right\|_{L_\infty} \leq C(1+t)^{-1/2} \tag{55}$$

for all $t \geq 0$, corresponding to the restriction on the small initial data $\int_{-\infty}^{\infty} u_0(x)\,dx \neq 0$. To confirm the numerical results, we verify that $u(x,t)$ approaches zero in the same decay rates. For instance, we use the same initial condition as equation (49) with $c = 0.03$, $x_0 = 0$, and $\alpha = 1$ with the space and time step sizes $h = 0.8$ and $\tau = h^2$. The simulations are run up to time $T = 5000$ over the region $[-100, 6500]$. The ratios $\|u^n\|/(1+t)^{-1/4}$ and $\|u^n\|_\infty/(1+t)^{-1/2}$ are presented as functions of time $t$ in Fig. 7, which are in agreement with equation (55).

## 5 Discussion

As we know, nonlinear schemes commonly trade with heavy computations. To break down the drawback, we introduce a fast numerical algorithm that requires only solving a constant matrix with a regular five-point stencil at a higher-time level, which is similar to the fourth-order schemes [30]. The important point is that our scheme can be iteratively solved and automatically saves a lot of computational costs, as shown in Tables 1 and 3 in the cases of the RLW and BBM–Burgers equations, respectively. According to Examples 1 and 2, the results suggest that the proposed scheme (Scheme I) is extraordinarily more accurate than Schemes II and III, which are constructed by classical approaches.

Additionally, the presented scheme is applied on the single solitary wave initial condition to study the effects of the viscous term $-\alpha u_{xx}$. The findings indicate that as the viscous coefficient increases, the wave amplitude decreases. Based on the numerical examples, it is inferred that the current scheme produces numerical results that correspond to physical phenomena by the RLW and BBM–Burgers equations. This has made a number of significant contributions to the field of numerical analysis to construct high-order FDMs for solving nonlinear PDEs.

## 6 Conclusion

In this study, we have successfully constructed and analyzed a three-level nonlinear implicit FDS for solving the RLW and BBM–Burgers equations, which were validated by numerical experiments and detailed theoretical analysis. The mass-conservative law is preserved by presented schemes in the different discrete sense. Utilizing boundedness analysis and a small temporal step size, the existence and uniqueness of the numerical solution can be directly estimated. The theoretical supports for the proposed scheme are also provided in terms of the stability and convergence of the numerical solution of order $O(\tau^2 + h^4)$. More precisely, the convergence rate turns into $O(\tau^4 + h^4)$ when $\alpha = 0$. These results have manifested that the present method is more productive and introduces a significant improvement for solving the BBM–Burgers equation. We expect that the results of this paper are useful for the understanding and numerical study of the shallow water equations, which will gain a lot of potentials to study real-world scenarios.

**Acknowledgements**

The authors would like to thank the reviewers for taking the time and effort necessary to review the manuscript. We sincerely appreciate all valuable comments and suggestions, which helped us to improve the quality of the manuscript. We also would like to thank the handling editors for the help in the processing of the paper.

**Funding**

This research was supported by the Centre of Excellence in Mathematics, Thailand, the Commission on Higher Education, Thailand, the National Research Council of Thailand (NRCT) under Grant No. N42A650208, and Chiang Mai University, Thailand.

**Availability of data and materials**
Not applicable.

## Declarations

**Competing interests**
The authors declare no competing interests.

**Author contributions**
All persons who meet authorship criteria are listed as authors, and all authors certify that they have participated sufficiently in the work to take public responsibility for the content, including participation in the concept, design, analysis, writing, or revision of the manuscript. Furthermore, each author certifies that this or similar material has not been and will not be submitted to or published in any other journal. All authors read and approved the final manuscript.

## Publisher's Note



Received: 25 March 2021 Accepted: 7 February 2023 Published online: 03 March 2023

**References**

1. Peregrine, D.H.: Calculations of the development of an undular bore. J. Fluid Mech. **25**, 321–330 (1966)
2. Peregrine, D.H.: Long waves on a beach. J. Fluid Mech. **27**, 815–827 (1967)
3. Boussinesq, J.V.: Essai sur la Théorie des Eaux Courantes (Essay on the theory of water flow). Mémoires présentés par divers savants a l'Academie des Sciences, Paris, France **23 (3) (1)** (1877). (in French)
4. Korteweg, D.J., de Vries, G.: On the change of form of long waves advancing in a rectangular canal, and on a new type of long stationary waves. Philos. Mag. **39**, 422–443 (1895)
5. Bona, J.L., Bryant, P.J.: A mathematical model for long waves generated by wave makers in nonlinear dispersive systems. Proc. Camb. Philos. Soc. **73**, 391–405 (1973)
6. Grimshaw, R.: Internal solitary waves. In: Environmental Stratified Flows (2002)
7. Apel, J.P.: A new analytical model for internal solitons in the ocean. J. Phys. Oceanogr. **33** 2247–2269 (2003)
8. Rottman, J.W., Grimshaw, R.: Atmospheric internal solitary waves. In: Environmental Stratified Flows (2002)
9. Chousurin, R., Mouktonglang, T., Wongsaijai, B., Poochinapan, K.: Performance of compact and non-compact structure preserving algorithms to traveling wave solutions modeled by the Kawahara equation. Numer. Algorithms **85**, 523–541 (2020)
10. Jain, P.C., Shankar, R., Singh, T.V.: Numerical solution of regularized long-wave equation. Commun. Numer. Methods Eng. **9**, 579–586 (1993)
11. Gardner, L.R.T., Gardner, G.A., Dogan, A.: A least-squares finite element scheme for the RLW equation. Commun. Numer. Methods Eng. **12**, 795–804 (1996)
12. Zaki, S.I.: Solitary waves of the split RLW equation. Comput. Phys. Commun. **138**, 80–91 (2001)
13. Dogan, A.: Numerical solution of RLW equation using linear finite elements within Galerkin's method. Appl. Math. Model. **26**, 771–783 (2002)
14. Raslan, K.R.: A computational method for the regularized long wave (RLW) equation. Appl. Math. Comput. **167**, 1101–1118 (2005)
15. Esen, A., Kutluay, S.: Application of a lumped Galerkin method to the regularized long wave equation. Appl. Math. Comput. **174**, 833–845 (2006)
16. Mei, L.Q., Chen, Y.P.: Numerical solutions of RLW equation using Galerkin method with extrapolation techniques. Comput. Phys. Commun. **183**, 1609–1616 (2012)
17. Cai, J., Gong, Y., Liang, H.: Novel implicit/explicit local conservative schemes for the regularized long-wave equation and convergence analysis. J. Math. Anal. Appl. **447**, 17–31 (2017)
18. Rouatbi, A., Omrani, K.: Two conservative difference schemes for a model of nonlinear dispersive equations. Chaos Solitons Fractals **104**, 516–530 (2017)
19. Zhang, L.: A finite difference scheme for generalized regularized long-wave equation. Appl. Math. Comput. **168**, 962–972 (2005)
20. Tamang, N., Wongsaijai, B., Mouktonglang, T., Poochinapan, K.: Novel algorithm based on modification of Galerkin finite element method to general Rosenau-RLW equation in (2 + 1)-dimensions. Appl. Numer. Math. **148**, 109–130 (2020)
21. Xiao, Q., Zhao, H.: Nonlinear stability of generalized Benjamin–Bona–Mahony–Burgers shock profiles in several dimensions. J. Math. Anal. Appl. **406**, 165–187 (2013)
22. Daghan, D., Donmez, O., Tuna, A.: Explicit solutions of the nonlinear partial differential equations. Nonlinear Anal., Real World Appl. **11**, 2152–2163 (2010)
23. Bruzon, M.S., Gandarias, M.L.: Conservation laws for a family of Benjamin–Bona–Mahony–Burgers equations. In: NSC 2012–4th IEEE International Conference on Nonlinear Science and Complexity August 6-11, Budapest, Hungary (2012)
24. Choi, J.H., Kim, H.: Bell-shaped and kink-shaped solutions of the generalized Benjamin–Bona–Mahony–Burger equation. Results Phys. **7**, 2369–2374 (2017)
25. Omrani, K., Ayadi, M.: Finite difference discretization of the Benjamin–Bona–Mahony–Burgers' equation. Numer. Methods Partial Differ. Equ. **24**(1), 239–248 (2008)
26. Cuesta, C.M., Pop, I.S.: Numerical schemes for a pseudo-parabolic Burgers' equation: discontinuous data and long-time behavior. J. Comput. Appl. Math. **224**(1), 269–283 (2009)

27. Che, H.-T., Pan, X.-T., Zhang, L.-M., Wang, Y.-J.: Numerical analysis of a linear-implicit average scheme for generalized Benjamin–Bona–Mahony–Burgers' equation. J. Appl. Math. **14**, Art. ID 308410 (2012)
28. Mohebbi, A., Faraz, Z.: Solitary wave solution of nonlinear Benjamin–Bona–Mahony–Burgers equation using a high-order difference scheme. Comput. Appl. Math. **36**, 915–927 (2017)
29. Zhao, X., Li, D., Shi, D.: A finite difference scheme for RLW-Burgers equation. J. Appl. Math. Inform. **26**, 573–581 (2008)
30. Bayarassou, K.: Fourth-order accurate difference schemes for solving Benjamin–Bona–Mahony–Burgers (BBMB) equation. Eng. Comput. **37**, 123–138 (2021)
31. Al-Khaled, K., Momani, S., Alawneh, A.: Approximate wave solutions for generalized Benjamin–Bona–Mahony–Burgers equations. Appl. Math. Comput. **171**(1), 281–292 (2005)
32. Mohammadi, M., Mokhtari, R.: Solving the generalized regularized long wave equation on the basis of a reproducing kernel space. J. Comput. Appl. Math. **235**(14), 4003–4014 (2011)
33. Dehghan, M., Abbaszadeh, M., Mohebbi, A.: The numerical solution of nonlinear high dimensional generalized Benjamin–Bona–Mahony–Burgers' equation via the meshless method of radial basis functions. Comput. Math. Appl. **68**(3), 212–237 (2014)
34. Zarebnia, M., Parvaz, R.: On the numerical treatment and analysis of Benjamin–Bona–Mahony–Burgers equation. Appl. Math. Comput. **284**, 79–88 (2016)
35. Kumar, R., Baskar, S.: B-spline quasi-interpolation based numerical methods for some Sobolev type equations. J. Comput. Appl. Math. **292**, 41–66 (2016)
36. Karakoc, S.B.G., Bhowmik, S.K.: Galerkin finite element solution for Benjamin–Bona–Mahony–Burgers equation with cubic B-splines. Comput. Math. Appl. **77**, 1917–1932 (2019)
37. Wang, T., Guo, B., Xu, Q.: Fourth-order compact and energy conservative difference schemes for the nonlinear Schrödinger equation in two dimensions. J. Comput. Phys. **243**, 382–399 (2013)
38. Hao, Z.P., Sun, Z.Z., Cao, W.R.: A three-level linearized compact difference scheme for the Ginzburg–Landau equation. Numer. Methods Partial Differ. Equ. **31**(3), 876–899 (2015)
39. Kerdboon, J., Yimnet, S., Wongsaijai, B., Mouktonglang, T., Poochinapan, K.: Convergence analysis of the higher-order global mass-preserving numerical method for the symmetric regularized long-wave equation. Int. J. Comput. Math. **98**(5), 869–902 (2021)
40. Zhou, Y.: Application of Discrete Functional Analysis to the Finite Difference Method. Inter. Acad. Publishers, Beijing (1990)
41. Sun, Z.Z., Zhu, Q.D.: On Tsertsvadze's difference scheme for the Kuramoto–Tsuzuki equation. J. Comput. Appl. Math. **98**, 289–304 (1998)
42. Wongsaijai, B., Mouktonglang, T., Sukantamala, N., Poochinapan, K.: Compact structure-preserving approach to solitary wave in shallow water modeled by the Rosenau-RLW equation. Appl. Math. Comput. **340**, 84–100 (2019)
43. Nanta, S., Yimnet, S., Poochinapan, K., Wongsaijai, B.: On the identification of nonlinear terms in the generalized Camassa–Holm equation involving dual-power law nonlinearities. Appl. Numer. Math. **160**, 386–421 (2021)
44. Wongsaijai, B., Poochinapan, K.: A three-level average implicit finite difference scheme to solve equation obtained by coupling the Rosenau-KdV equation and the Rosenau-RLW equation. Appl. Math. Comput. **245**, 289–304 (2014)
45. He, D., Pan, K.: A linearly implicit conservative difference scheme for the generalized Rosenau–Kawahara-RLW equation. Appl. Math. Comput. **271**, 323–336 (2015)
46. He, D.: New solitary solutions and a conservative numerical method for the Rosenau–Kawahara equation with power law nonlinearity. Nonlinear Dyn. **82**, 1177–1190 (2015)
47. Wang, X., Dai, W.: A three-level linear implicit conservative scheme for the Rosenau-KdV-RLW equation. J. Comput. Appl. Math. **330**, 295–306 (2018)
48. Mei, M.: Large-time behavior of solution for generalized Benjamin–Bona–Mahony–Burgers equations. Nonlinear Anal., Theory Methods Appl. **33**, 699–714 (1998)
49. Mei, M.: $L_q$-Decay rates of solutions for Benjamin–Bona–Mahony–Burgers equations. J. Differ. Equ. **158**, 314–340 (1999)
50. Mei, M.: Long-time behavior of solution for Rosenau–Burgers equation (I). Appl. Anal. **63**, 315–330 (1996)